

**Elevated free fatty acid uptake via CD36 promotes epithelial-mesenchymal transition in hepatocellular carcinoma**

Aritro Nath<sup>1</sup>, Irene Li<sup>2</sup>, Lewis R. Roberts<sup>3</sup> and \*Christina Chan<sup>1, 2, 4</sup>

<sup>1</sup> Genetics Program, Michigan State University, 567 Wilson Road, Rm 2240E, East Lansing, Michigan 48824, USA

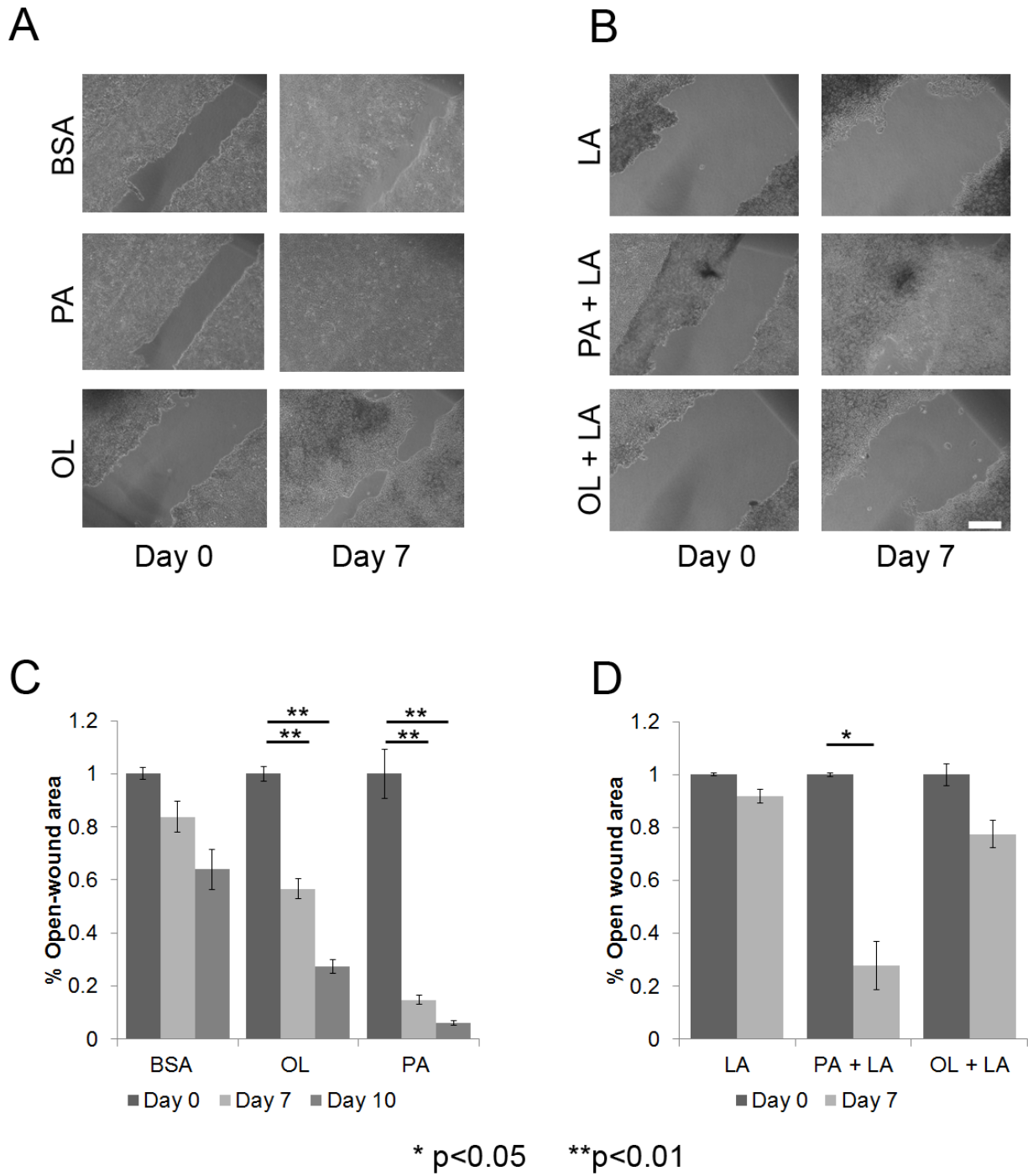
<sup>2</sup> Department of Microbiology and Molecular Genetics, Michigan State University, 567 Wilson Road, Rm 2215, East Lansing, Michigan 48824, USA

<sup>3</sup> Division of Gastroenterology and Hepatology, Mayo Clinic College of Medicine, 200 First St. SW, Rochester, Minnesota 55905, USA

<sup>4</sup> Department of Chemical Engineering and Materials Science, Michigan State University, 428 South Shaw Lane, Rm 2527, East Lansing, Michigan 48824, USA

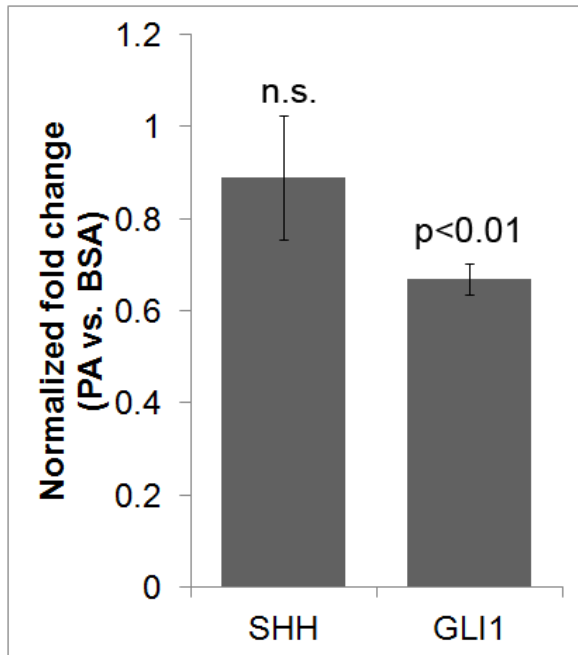
\*Corresponding author

[krischan@egr.msu.edu](mailto:krischan@egr.msu.edu)



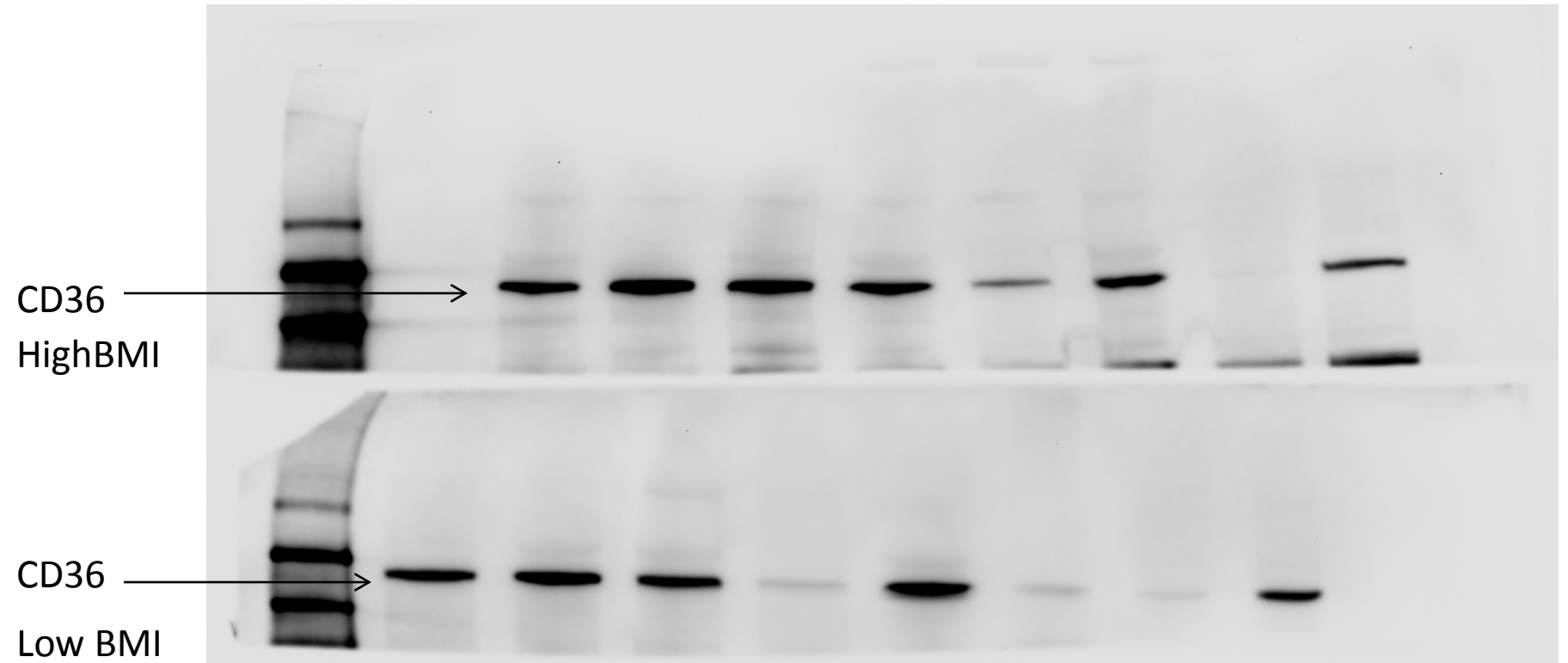
**Supplementary Figure 1: Differential effects of FFAs on migration.** A & B. Scratch-wound healing assays. HepG2 cells were grown to 80% confluence in regular medium, and a scratch was introduced on the monolayer. The cells were then cultured in regular media containing either

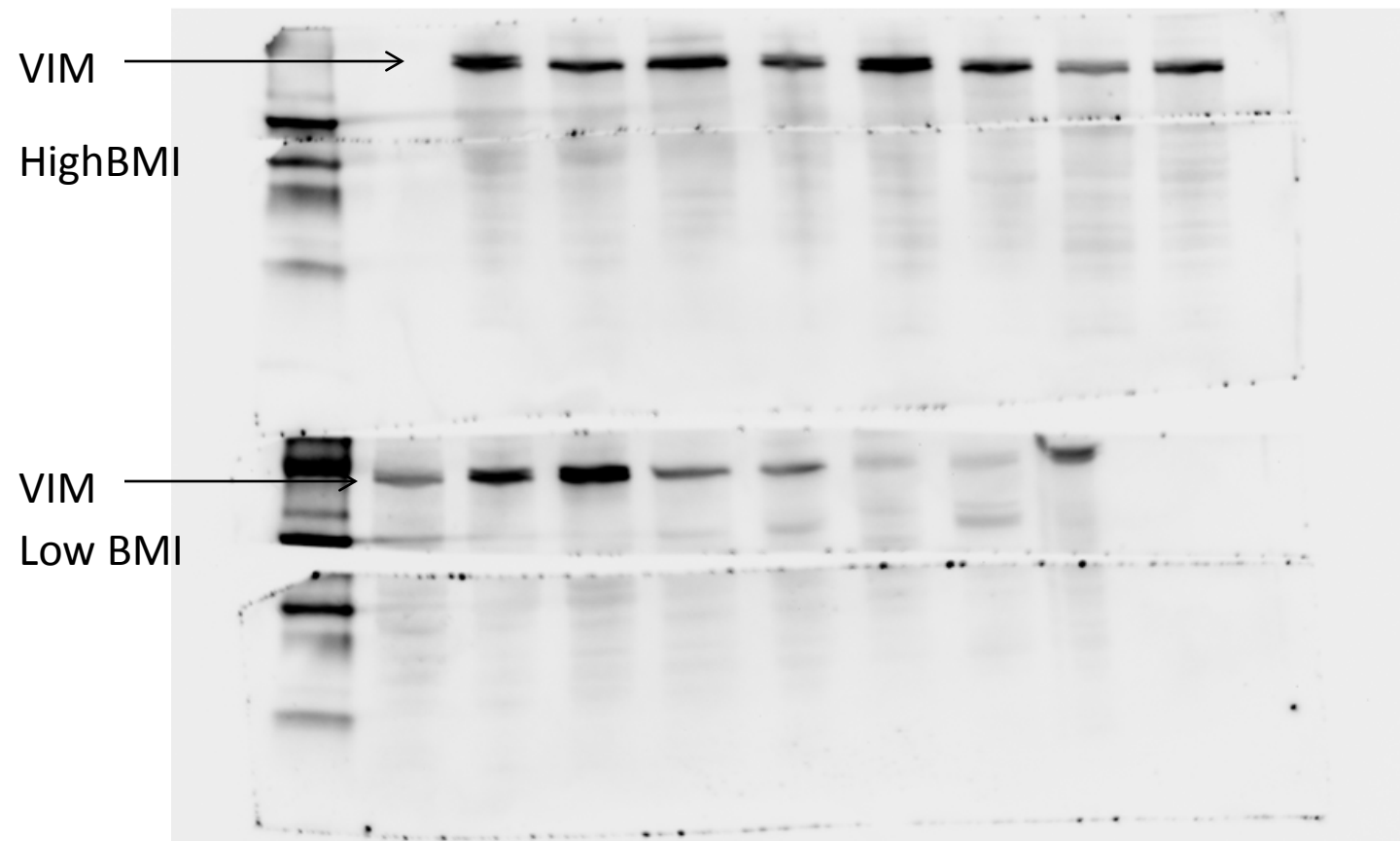
BSA (control), PA (0.4mM), OL (0.4mM), LA (0.4mM), PA (0.2mM) + LA (0.2mM) or OL (0.2mM) + LA (0.2mM). The migration of the wound front was monitored over a 10-day period to establish an empirical time-frame within which the cell front acquired the ability to migrate across the wound. Phase contrast images were recorded at 40X magnification (scale bar=50 $\mu$ m) C & D. Bar graph showing the open wound area in treated cells calculated using the T-scratch package at different time points normalized to open wound area at 0 hr. P-values indicate significance levels (n=3) determined by Student's t-test (two tailed).



**Supplementary Figure 2** mRNA expression levels of Hedgehog ligand *SHH* and downstream transcription factor *GLI1* in PA vs. BSA treated HepG2 cells. Bar graphs showing fold-change in *GAPDH* normalized expression levels of *SHH* and *GLI1* in PA vs. BSA treated HepG2 cells. P-value indicates comparison of average delta Ct values between PA and BSA using two tailed Student's t-test.

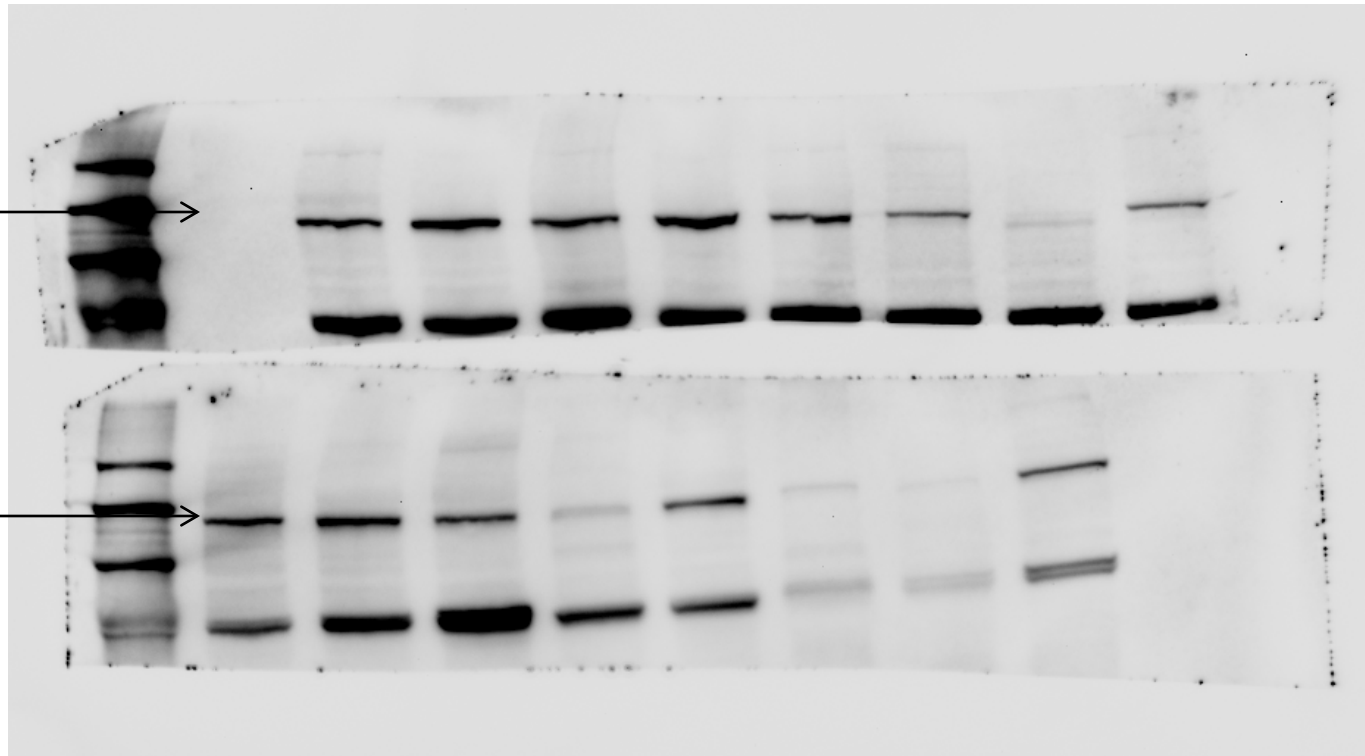
# Supplementary Figure 3





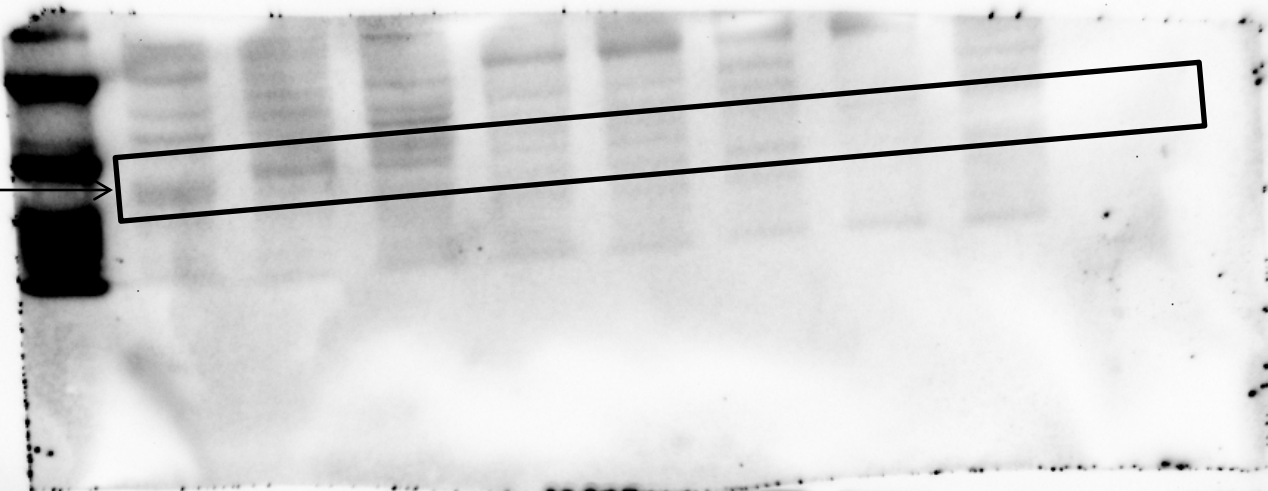
CDH1 →  
High BMI

CDH1 →  
Low BMI



40  
30  
20

SNAIL  
Low BMI

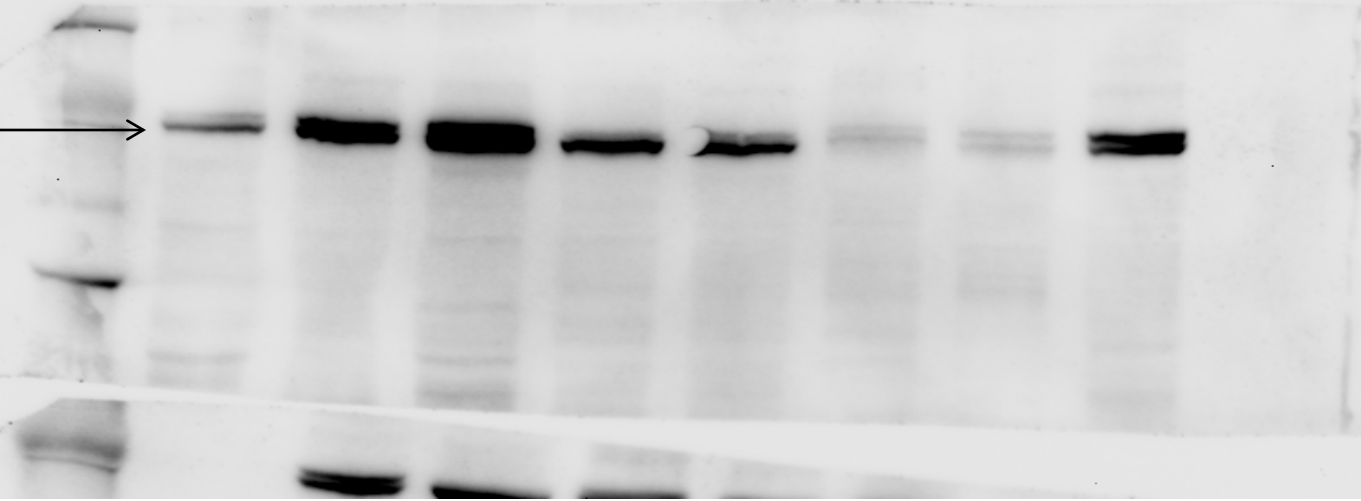
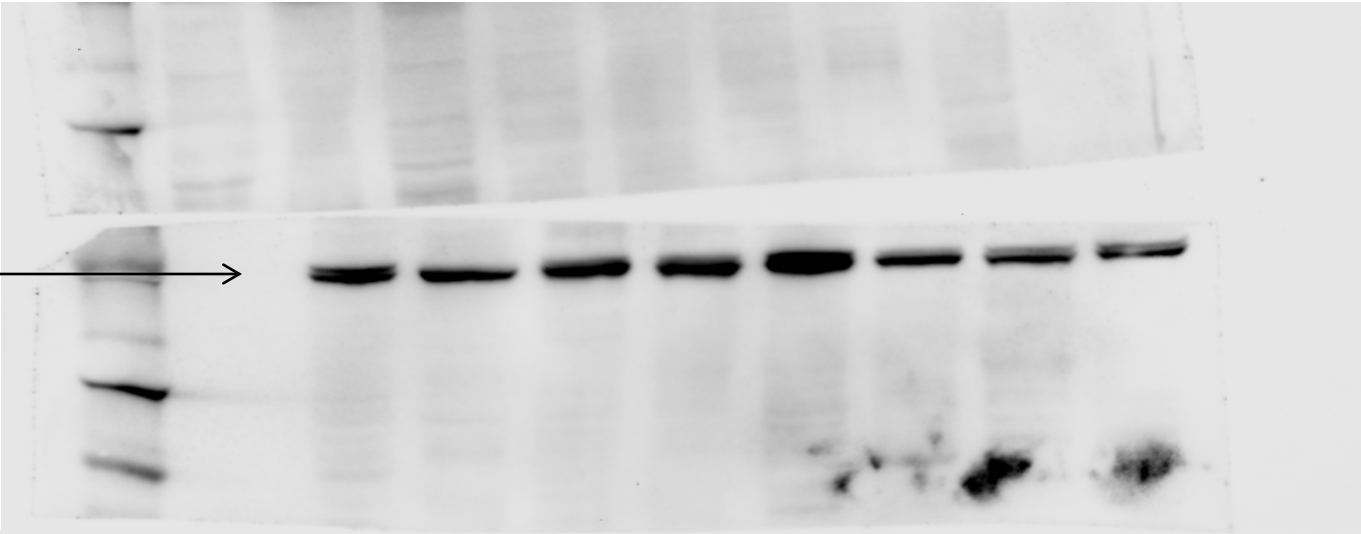


40  
30  
20

SNAIL  
High BMI





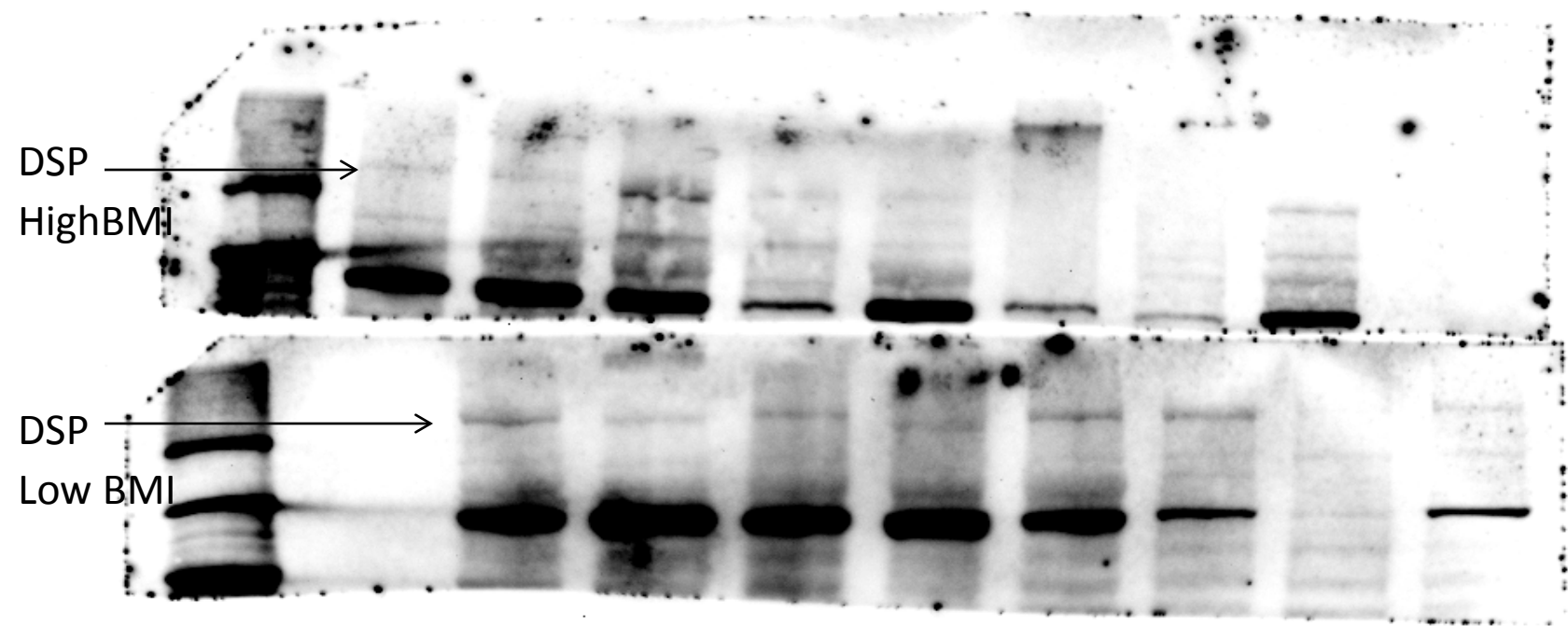


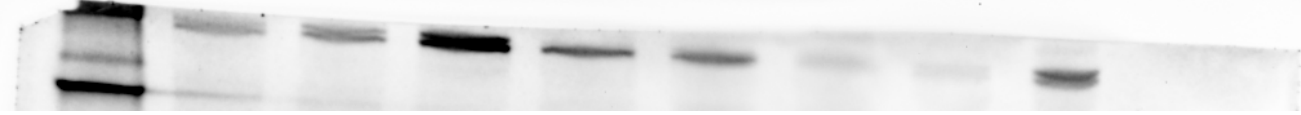
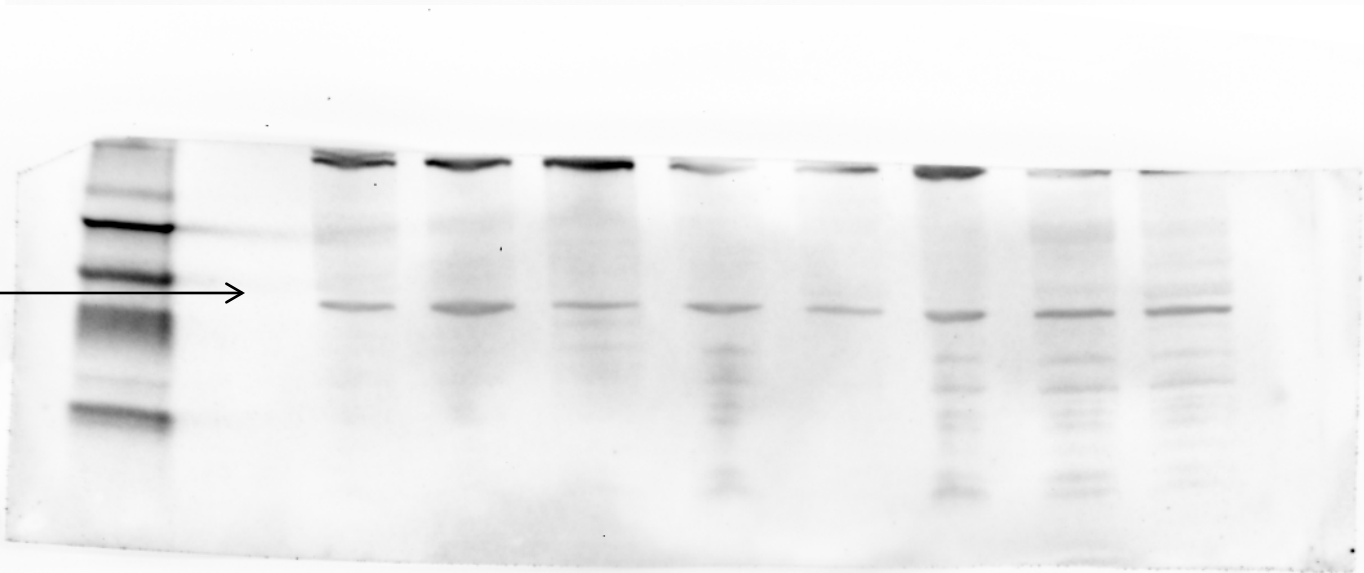
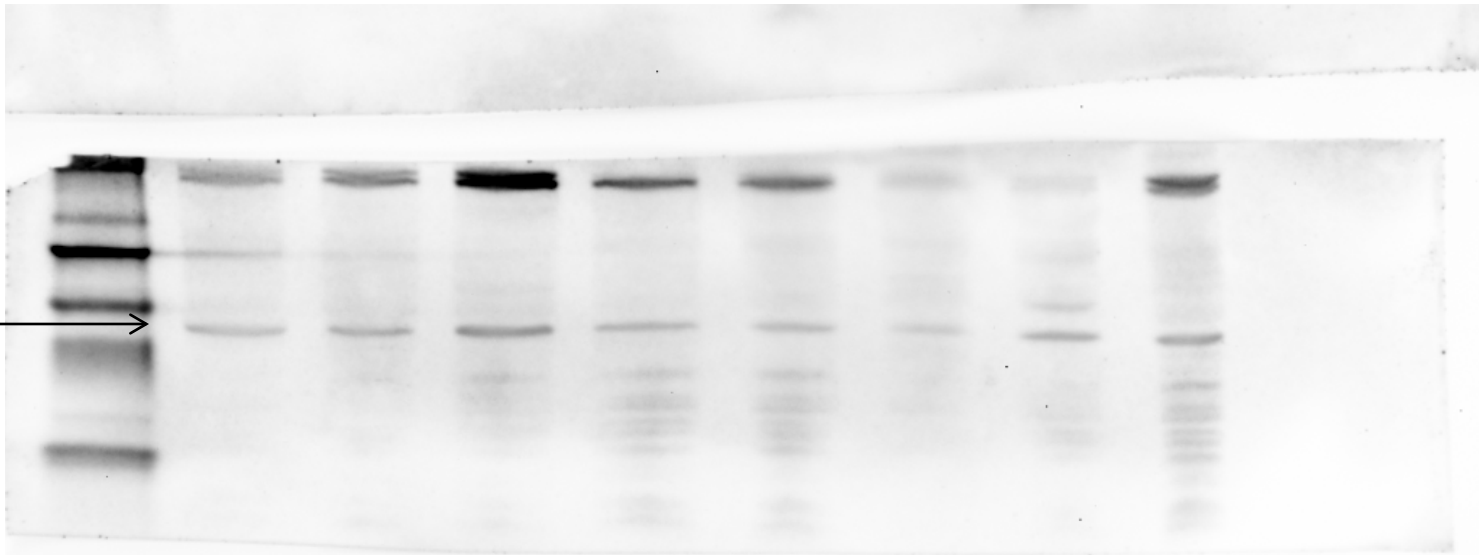
PORCN →

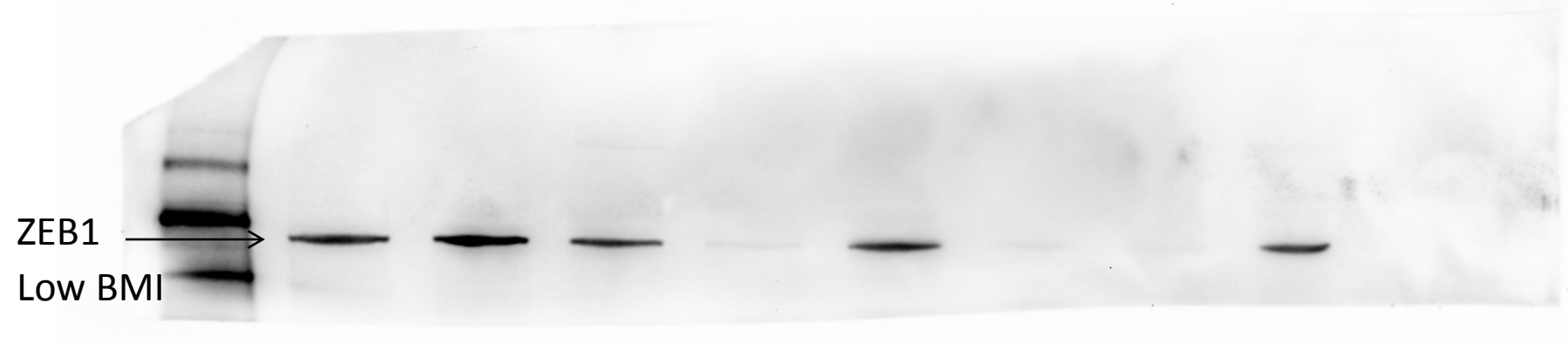
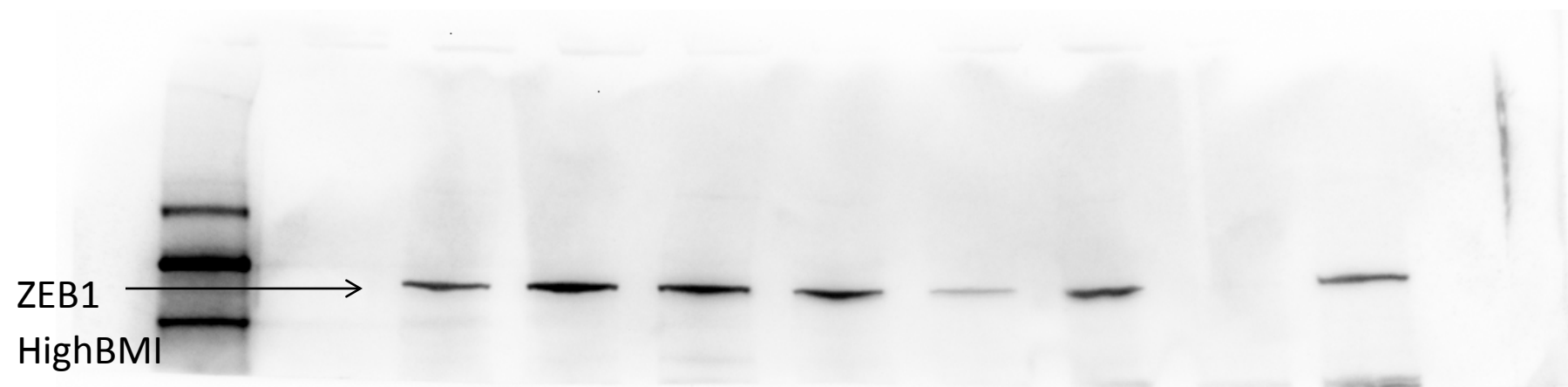
High BMI

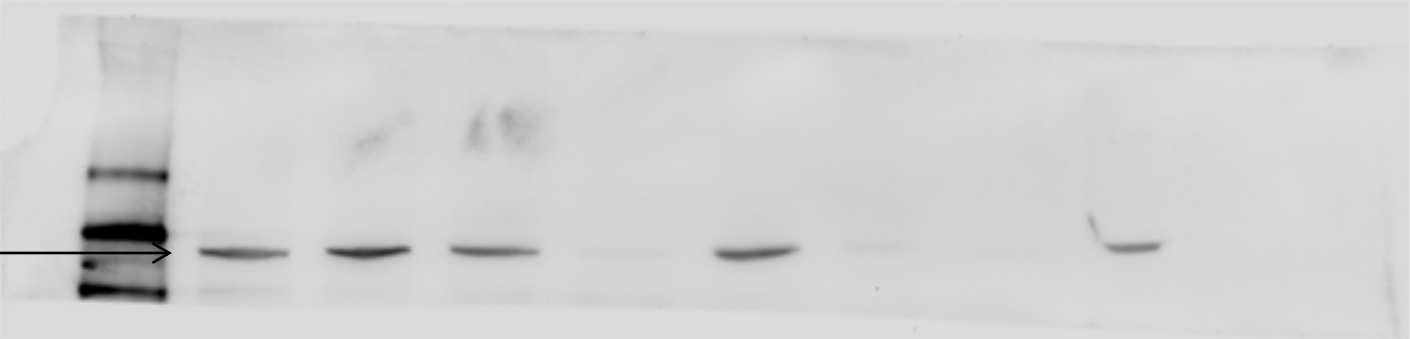
PORCN →

Low BMI



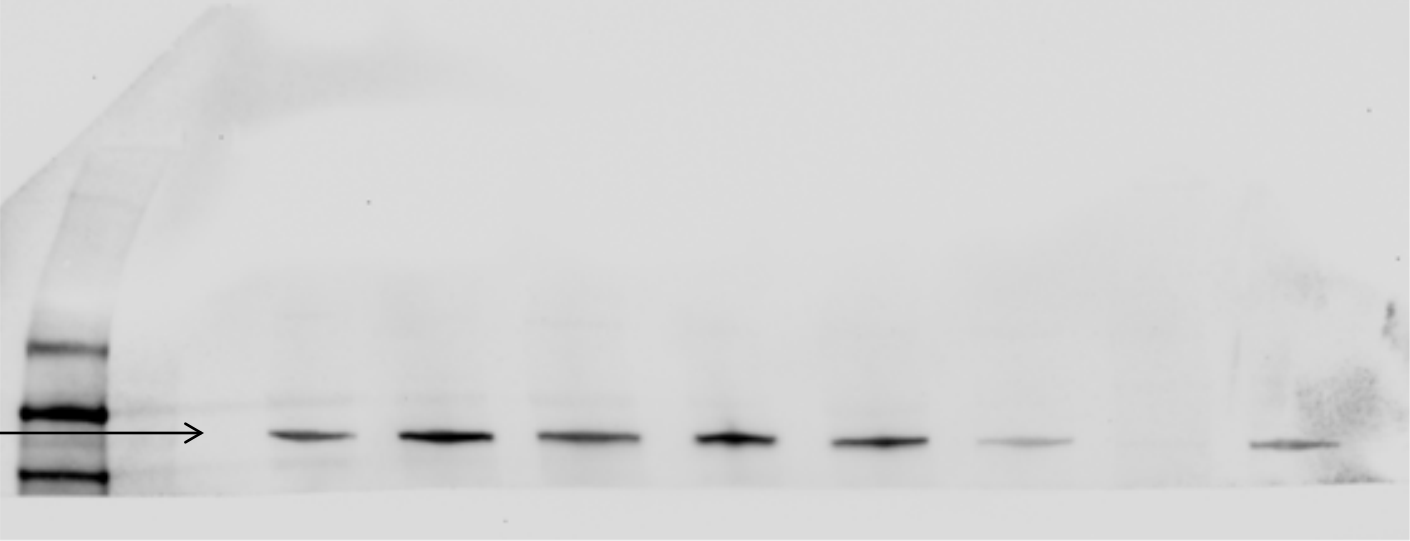






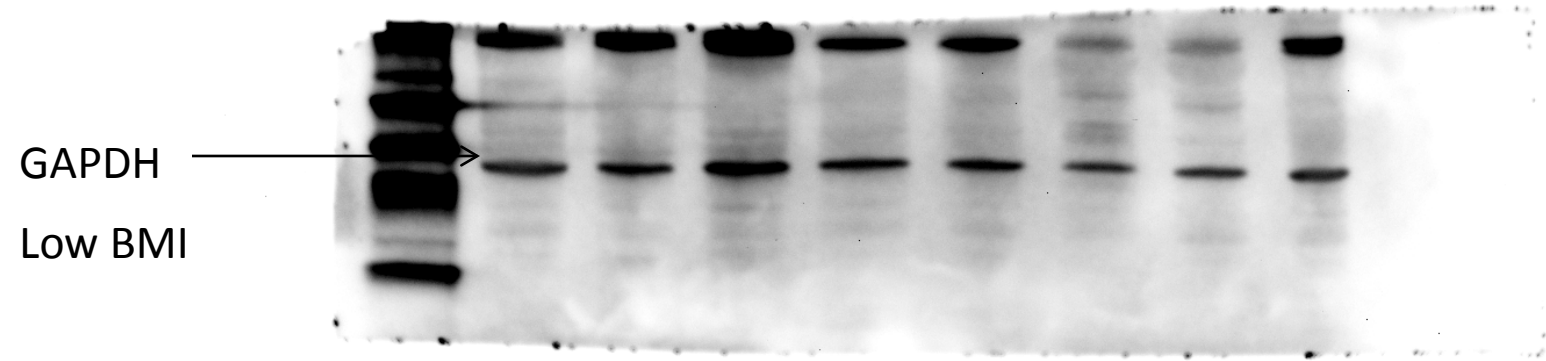
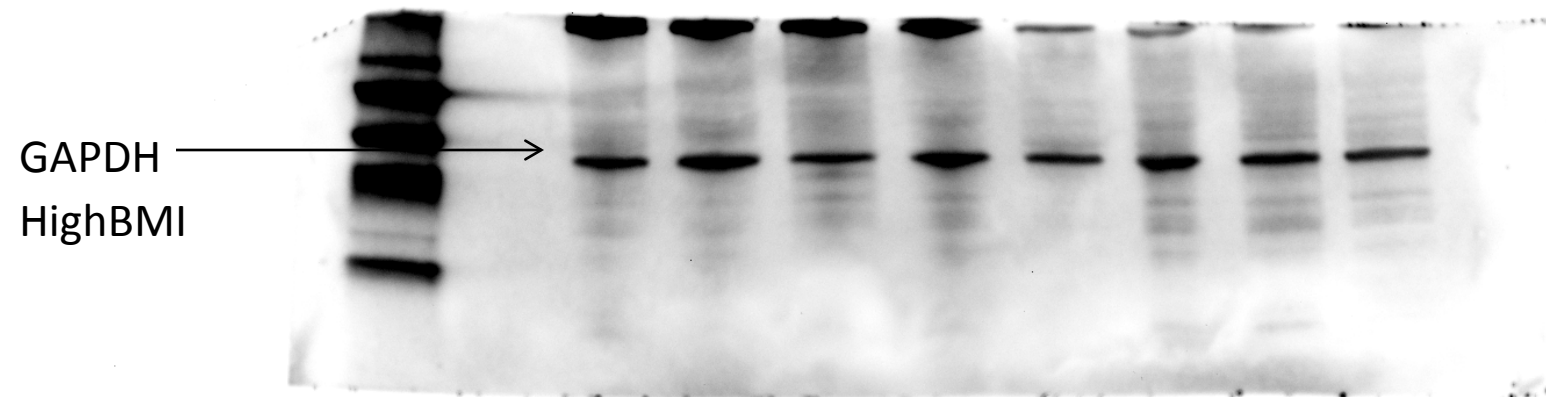
ZEB2

Low BMI



ZEB2

High BMI



# Supplementary Figure 4

+SSO

-SSO

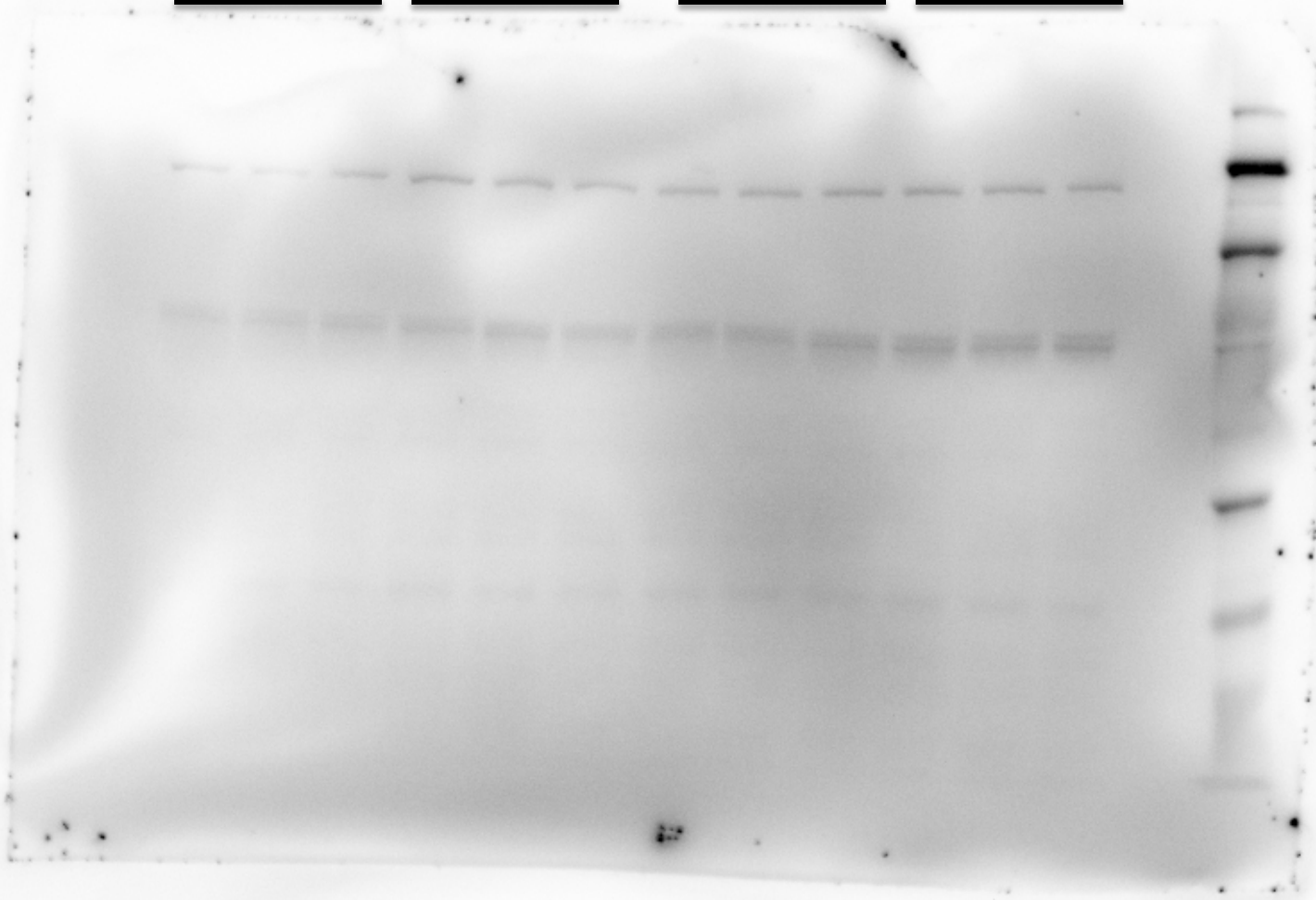
PA

BSA

PA

BSA

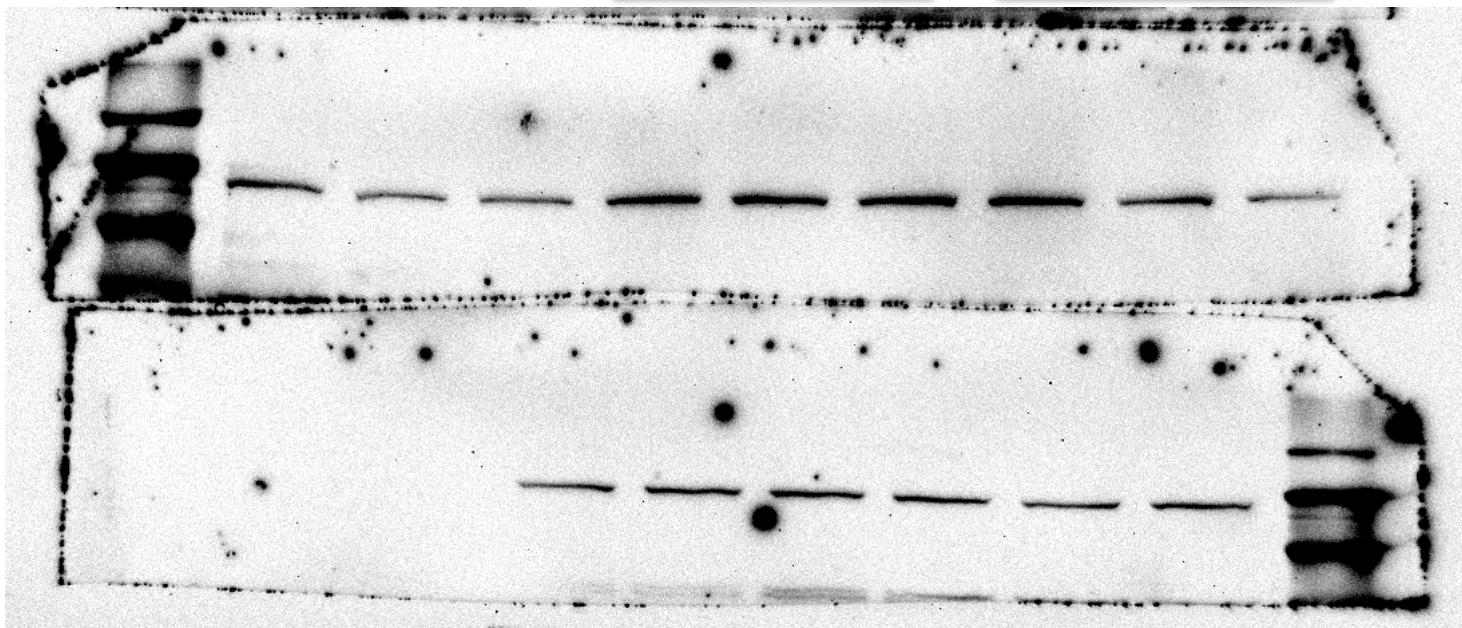
VIM



-SSO

BSA

PA



CDH1

CDH1

PA

BSA

+SSO



-SSO

BSA

PA

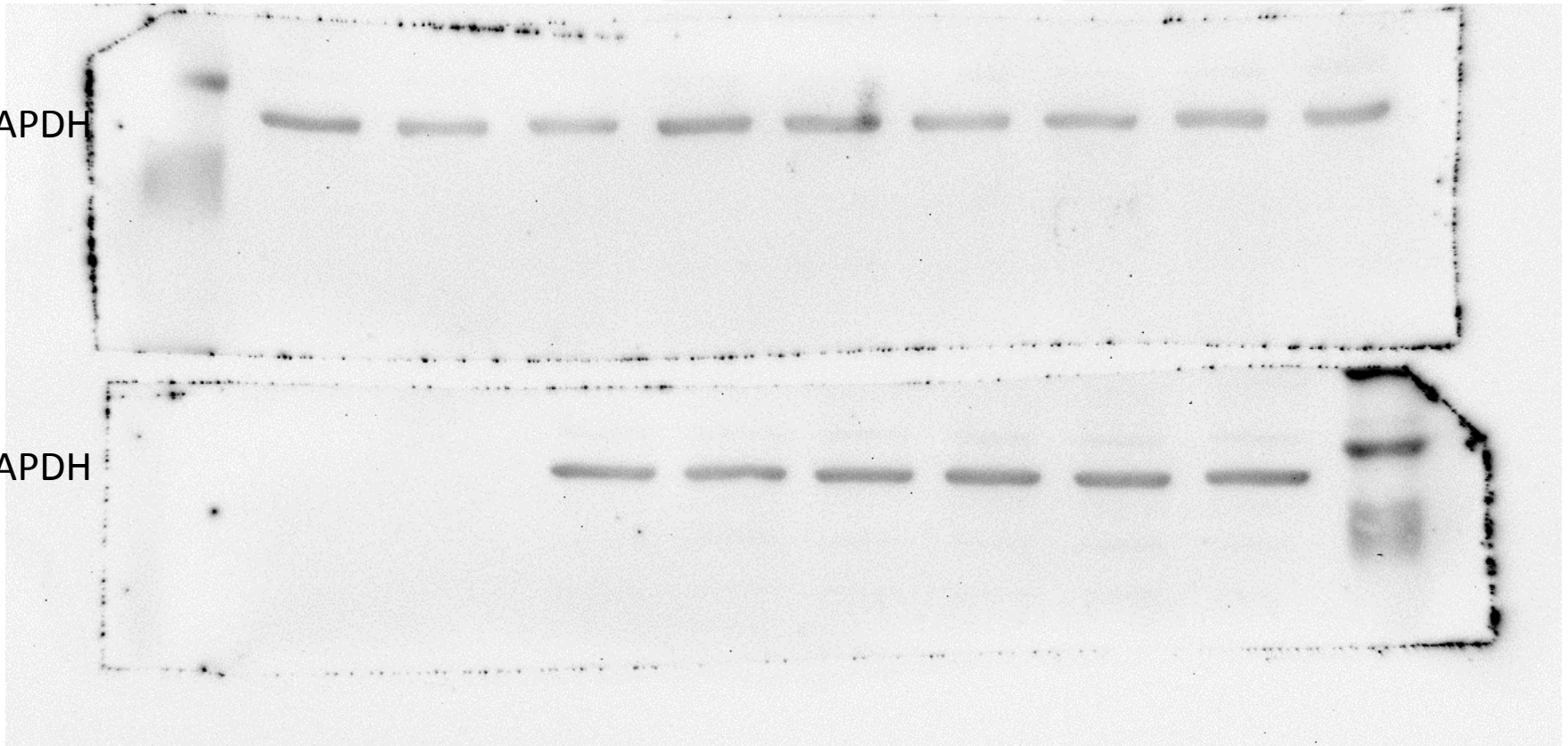
GAPDH

GAPDH

PA

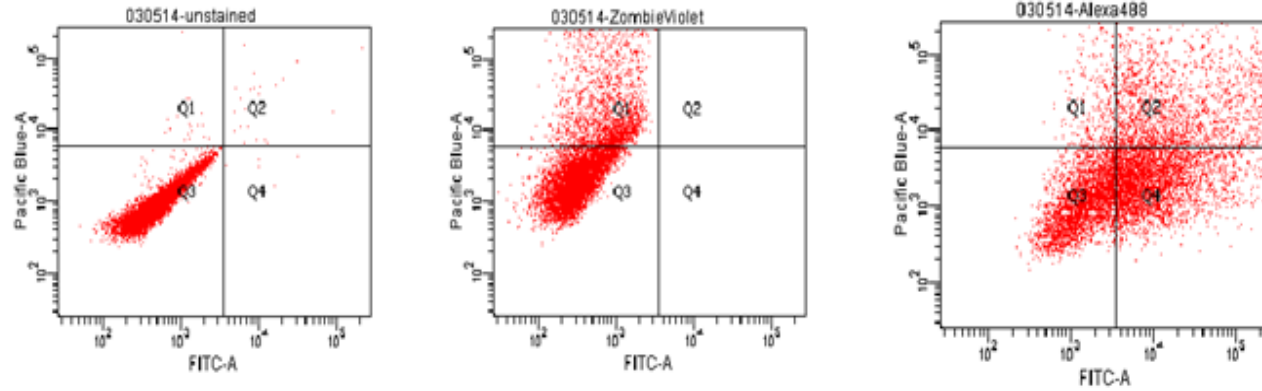
BSA

+SSO

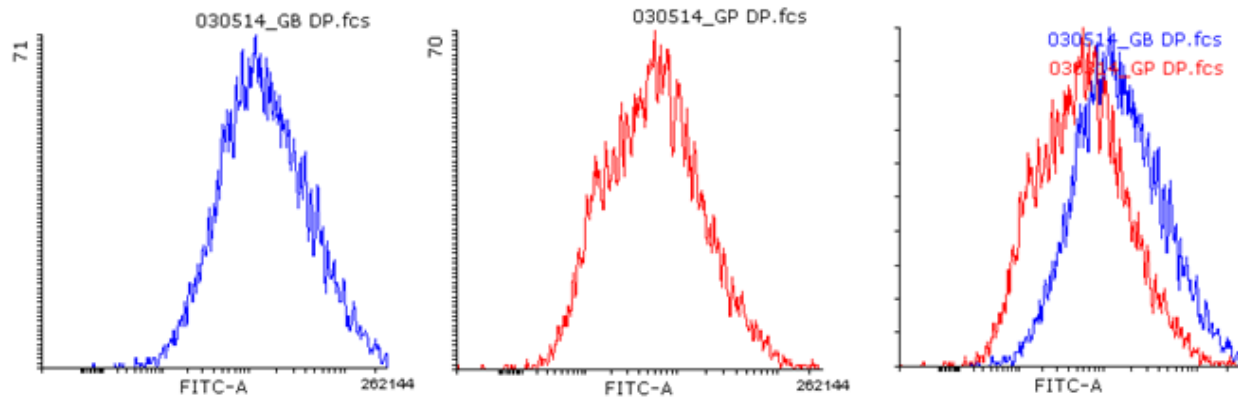


# Supplementary Figure 5

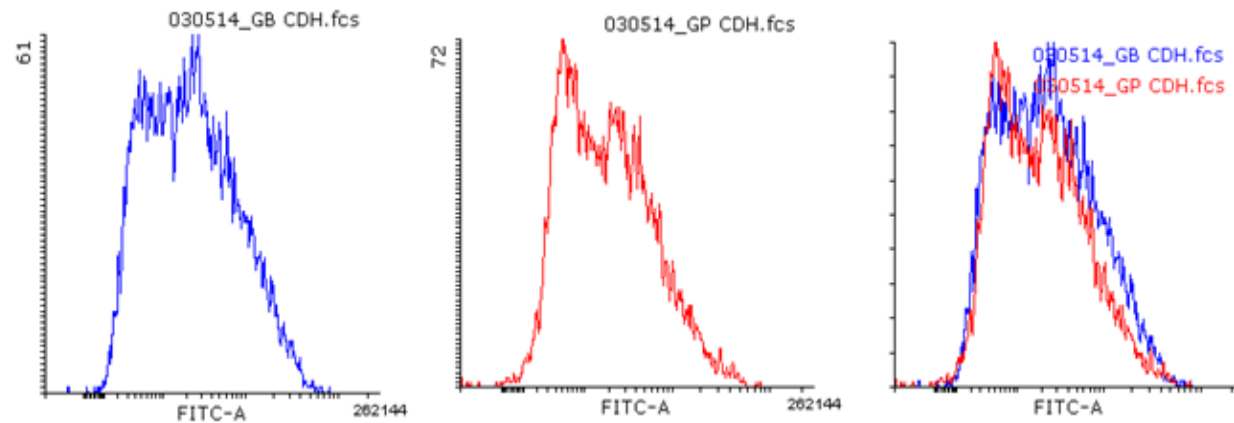
**A**



**B**



**C**



**Supplementary Figure 5: A.** (From left to right) Panels showing unstained control to set gating threshold Zombie Violet stained cells and GAPDH-Alexa488 stained cells. This gating was used for the subsequent marker assessment. The plot distributions show the signal intensity distributions for **B.** DSP and **C.** CDH1 from BSA (BLUE) or PA (RED) treated cells. The overlap images show that the DSP peak in the PA treated cells is clearly shifted towards the left, indicating a population of cells with reduced DSP expression in PA treated condition. The CDH1 plots show a distinct bi-modal distribution, where the low-intensity peak (lower CDH expression) is higher in the PA treated cells, while the high-intensity peak (higher CDH expression) is higher in the control cells, and is suggestive of sub-population of cells.





**Supplementary Table 3**

Patient clinical information								Western Blot quantification								
TSS ID	BMI	SEX	Grade	T	N	M	STAGE	CD36	VIM	ZEB1	ZEB2	TGFB	PORCN	CDH	DSP	SNAIL
Patient Key:6680	16.28	M	3	2	0	0	II	1.18	0.64	0.67	0.74	0.39	0.24	0.34	0.34	0.38
Patient Key: 3993	19.89	F	2	3	0	0	III	1.81	1.72	1.18	1.26	0.46	2.59	0.88	0.20	0.24
Patient Key:2604	21.6	F	2	1	0	0	I	1.00	1.77	0.42	0.52	0.68	2.11	0.34	0.13	0.05
Patient Key:5828	21.75	M	3	3	0	0	III	0.09	0.63	0.01	0.02	0.30	1.08	0.07	0.08	0.00
Patient Key:3167	22.77	M	3	3A	0	1	IV	1.51	0.57	0.66	0.74	0.28	1.10	0.40	0.28	0.02
Patient Key:5858	22.82	M	2	1	0	0	I	0.08	0.13	0.01	0.01	0.13	0.09	0.03	0.24	0.04
Patient Key:2613	23.63	F	3	2	0	0	II	0.01	0.09	0.00	0.01	0.32	0.06	0.01	0.00	0.00
Patient Key:3013	23.77	M	3	3	0	0	IIIA	0.60	0.39	0.33	0.23	0.36	1.49	0.27	0.09	0.00
Patient Key: SW1	36.05	F	2	3	0	0	IIIA	1.64	2.24	0.69	0.68	0.86	2.17	0.73	0.11	0.76
Patient Key: 8118	35.14	M	2	3A	X	0	X	1.26	0.93	0.73	0.79	0.84	1.03	0.58	0.04	0.30
Patient Key: 10316	35.45	F	1	2	X	X	X	2.28	2.27	1.27	1.04	0.50	2.33	0.75	0.67	0.00
Patient Key:4068	35.49	M	3	1	0	0	I	1.15	0.91	0.69	0.82	0.61	1.54	0.68	0.05	0.14
Patient Key:3423	37.66	M	2	1	0	0	I	0.85	2.76	0.20	1.12	0.52	3.37	0.58	0.09	0.12
Patient Key: SW14	39.97	M	1	3	0	0	IIIA	1.56	1.49	0.70	0.16	0.76	1.40	0.21	0.00	1.63
Patient Key: 6796	35.32	F	3	2	1	0	IIIC	0.01	0.68	0.00	0.00	0.72	1.10	0.02	0.00	0.31
Patient Key: 3070	36.04	M	3	3	0	X	X	1.03	1.21	0.54	0.29	0.86	0.91	0.19	0.06	0.25

**TSS ID**                      **Hx of disease**  
Patient Key:6680            chronic HBV; dx with HCC 6/2/2009; HCC recurrence on 12/3/2009;  
Patient Key: 3993            dx with HCC 7/23/1996; recurrence on 10/15/1996  
Patient Key:2604            extreme smoking until 1996, dx with HCC w/o Cirrhosis 5/7/2001, recurrence 10/1/2002, recurrence 05/14/2003  
Patient Key:5828            Chronic HBV; dx with HCC 05/29/2008; Metastatic HCC to lung 4/8/2009  
Patient Key:3167            Chronic HBV; dx with HCC 4/8/2003;  
Patient Key:5858            Chronic HBV: dx with cirrhosis in 2000, dx with HCC 6/13/2008;  
Patient Key:2613            Smoking history for 45 yrs; occasional alcohol consumption; dx with HCC 2006; recurrence of HCC 2010;  
Patient Key:3013            Chronic HCV; dx with HCC 1/18/2002; Metastatic HCC to sternum 10/19/2004  
Patient Key: SW1            dx with HCC 2/9/2004  
Patient Key: 8118            remote alcohol history; dx with HCC 1/10/2011  
Patient Key: 10316            Chronic HCV; advance fibrosis; dx with HCC in 2012; recurrent HCC 5/6/2014; HCC with Cirrhosis 5/7/2014  
Patient Key:4068            dx with HCC 2/27/2006  
Patient Key:3423            nonalcoholic steatohepatitis with cirrhosis; dx with HCC 5/31/2005  
Patient Key: SW14            dx with HCC 2007  
Patient Key: 6796            dx with CCA 6/11/2009 then determined to be HCC 6/27/2009;  
Patient Key: 3070            Heavy alcohol use; dx with HCC 6/25/2002;

**TSS ID**                      **Treatment history**  
Patient Key:6680            resection in 6/22/2009;  
Patient Key: 3993            resection in 7/23/1996; alcohol ablation in 10/17/1996; Chemoembolization 4/9/1997  
Patient Key:2604            hepatectomy in 5/14/2001; alcohol ablation 10/2/2002; alcohol ablation 05/15/2003  
Patient Key:5828            embolization 6/4/2008; treated with entecavir for HBV 5/52/2008; right hepatectomy & left portal vein thrombectomy 7/1/2008; Radiofrequency ablation 11/4/2008; Sorafenib 6/24/2009, Sorafenib+doxorubicin 1/5/2010, Sorafenib only 6/22/2010; MC0812 Chemotherapy (Cisplatin, gemcitabine, and everolimus) 11/11/2010; Cisplatin & Gemcitabine only 3/3/2011; Pazopanib & everolimus 7/24/2012  
Patient Key:3167            embolization right portal vein 4/14/2003; Hepatectomy, right adrenalectomy, & cholecystectomy 5/6/2003  
Patient Key:5858            portal embolization on the right hepatic lobe 6/17/2008  
Patient Key:2613            resection 2006 & 2010; laser ablation 10/14/2011, 6/7/2012, 9/20/2012, 10/4/2012, & 7/24/2013; Radiofrequency 10/28/2013; MR guided liver cyroablation 6/25/2014; MR cyroablation 1/7/2015;  
Patient Key:3013            Lamivudine 1/18/2002; resection 1/21/2002; Epiriv 5/28/2002;  
Patient Key: SW1            right hepatectomy 2/26/2004; TheraSphere treatment 8/31/2006; Hospice care 3/21/2007  
Patient Key: 8118            resection 1/14/2011;  
Patient Key: 10316            resection 9/2012; ethanol ablation 5/13/2014  
Patient Key:4068            right hepatectomy 3/3/2006  
Patient Key:3423            resection 6/7/2005  
Patient Key: SW14            resection 6/2007  
Patient Key: 6796            resection 6/24/2009  
Patient Key: 3070            resection 7/8/2002

Supplementary Table 4

HepG2	PA vs. BSA fold-change	Transcriptional regulation by TGF- $\beta$	Transcriptional regulation by WNT/ $\beta$ -catenin	Hep3B	PA vs. BSA fold-change	Transcriptional regulation by TGF- $\beta$	Transcriptional regulation by WNT/ $\beta$ -catenin
AHNAK	14.091	x		IL1RN	3.024		
COL5A2	3.672	x		MST1R	2.335		
WNT5B	3.630	x		TGFB2	2.194	x	
WNT11	3.095			SNAI3	2.174		
BMP2	2.745			TGFB3	2.033		
IL1RN	2.567			IGFBP4	1.995	x	
PPPDE2	2.555			ZEB2	1.858		
NODAL	2.520			BMP7	1.741		
FOXC2	2.479	x		NUDT13	1.617		
SOX10	2.229			SMAD2	1.576		
TSPAN13	2.204			TCF4	1.569	x	x
STEAP1	2.056			RGS2	1.562		
TGFB2	1.973	x		CDH2	1.558	x	
CDH1	1.950	x		COL3A1	1.555	x	
CALD1	1.749	x		SPP1	1.551		
MST1R	1.741			ESR1	1.548	x	
WNT5A	1.741	x		CALD1	1.491	x	
KRT7	1.709			CTNNB1	1.481	x	
VIM	1.606			GSK3B	1.468	x	
COL3A1	1.591	x		ILK	1.468		
MSN	1.569			TSPAN13	1.468		
ZEB2	1.562			PTP4A1	1.464		
MMP9	1.544			FGFBP1	1.447		
KRT19	1.488			VCAN	1.431		
SPARC	1.488			GNG11	1.418		
MMP3	1.485			GSC	1.418		
BMP7	1.478			TWIST1	1.418		
COL1A2	1.478			MAP1B	1.404		
GNG11	1.478			ZEB1	1.404		
GSC	1.478			PDGFRB	1.376		
TWIST1	1.478			SIP1	1.363		
PDGFRB	1.451			BMP1	1.357		
MMP2	1.414			F11R	1.357		
IGFBP4	1.408			EGFR	1.347		
VCAN	1.395			ITGAV	1.338		
TMEM132	1.382			PTK2	1.335		
OCLN	1.323			OCLN	1.326		
TFPI2	1.320			COL1A2	1.320		
SNAI3	1.310			COL5A2	1.281		
TCF4	1.301			KRT19	1.281		
MAP1B	1.298			KRT14	1.278		
ILK	1.295			TIMP1	1.275		
PTK2	1.260			SOX10	1.269		
RGS2	1.260			ITGA5	1.263		
NUDT13	1.251			PPPDE2	1.260		
FGFBP1	1.248			RAC1	1.260		
BMP1	1.243			STEAP1	1.254		
CTNNB1	1.243			MSN	1.248		
STAT3	1.214			STAT3	1.248		
AKT1	1.209			ITGB1	1.243		
F11R	1.209			ERBB3	1.228		
ERBB3	1.203			MMP9	1.223		
VPS13A	1.195			JAG1	1.200		
KRT14	1.187			AKT1	1.181		
SIP1	1.181			VPS13A	1.176		
TIMP1	1.178			NOTCH1	1.159		
PLEK2	1.176			DSP	1.157		
ITGA5	1.170			TCF3	1.151		
GSK3B	1.143			SNAI2	1.149		
TMEFF1	1.143			MMP2	1.146		
ITGB1	1.141			VIM	1.141		
SPP1	1.123			TFPI2	1.133		
TCF3	1.084			BMP2	1.128		
SMAD2	1.057			FN1	1.123		
CDH2	1.050			DSC2	1.117		
PTP4A1	1.050			WNT5B	1.110		
ESR1	1.043			NODAL	1.087		
FZD7	1.033			TMEM132	1.077		
ZEB1	1.028			CAV2	1.072		
SNAI1	1.026			CAMK2N1	1.062		
DSC2	1.009			TGFB1	1.045		
RAC1	1.005			SPARC	1.014		
JAG1	-1.019			PLEK2	1.007		
DSP	-1.069			CDH1	1.002		
TGFB1	-1.077			TMEFF1	-1.005		
SERPINE1	-1.102			SNAI1	-1.074		
FN1	-1.125			FZD7	-1.130		
CAMK2N1	-1.133			KRT7	-1.151		
NOTCH1	-1.178			WNT5A	-1.200		
ITGAV	-1.248			FOXC2	-1.376		
CAV2	-1.257			MMP3	-1.488		
TGFB3	-1.335			WNT11	-1.936		
SNAI2	-1.481			SERPINE1	-1.991		
EGFR	-2.047			AHNAK	-2.104		

Genes used for KEGG pathway enrichment analysis

Supplementary Table 5

CD36 vs TGFβ signaling (KEGG)				CD36 vs WNT signaling (KEGG)				CD36 vs PPARG/TFs			
Gene	Pearson's Correlation	P-value	FDR (BH)	Gene	Pearson's Correlation	P-value	FDR (BH)	Gene	Pearson's Correlation	P-value	FDR (BH)
CD36	1.000	0.002	0.013	CD36	1.000	0.002	0.014	CD36	1.000	0.002	0.005
BMP4	0.407	0.002	0.013	NKD1	0.568	0.002	0.014	PPARG	0.349	0.002	0.005
ROCK2	0.329	0.002	0.013	ANKK2	0.474	0.002	0.014	NFKB1	0.233	0.002	0.005
BMP9B18	-0.087	0.002	0.013	CTNNA1	0.414	0.002	0.014	NR1H2	-0.196	0.002	0.005
AMH	-0.143	0.002	0.013	TCF7	0.384	0.002	0.014	PPARA	0.296	0.006	0.013
COMP	-0.149	0.002	0.013	DAAH1	0.360	0.002	0.014	HIF1A	0.209	0.014	0.026
THBS2	-0.158	0.002	0.013	ROCK2	0.329	0.002	0.014	FOS	0.190	0.032	0.050
DCN	-0.165	0.002	0.013	PRKCA	0.303	0.002	0.014	NR1H2	0.065	0.341	0.469
BMP8B	-0.197	0.002	0.013	SFRP5	-0.093	0.002	0.014	PPARG	0.045	0.511	0.562
TGFβ1	-0.200	0.002	0.013	WNT9A	0.000	0.002	0.014	JUN	-0.058	0.499	0.562
INHBE	-0.203	0.002	0.013	PLCB4	-0.113	0.002	0.014	STAT3	0.005	0.932	0.932
BMP8A	-0.204	0.002	0.013	WNT2	-0.129	0.002	0.014				
ID2	-0.205	0.002	0.013	FZD1	-0.130	0.002	0.014				
LEFTY1	-0.154	0.004	0.023	MMMP7	-0.130	0.002	0.014				
SMAD5	-0.169	0.004	0.023	WNT7B	-0.139	0.002	0.014				
GDF5	0.386	0.006	0.030	WNT10A	-0.145	0.002	0.014				
SMAD3	0.203	0.006	0.030	FZD7	-0.147	0.002	0.014				
TGFβ2	0.197	0.008	0.034	WNT4	-0.178	0.002	0.014				
ID1	-0.135	0.008	0.034	NKD2	-0.184	0.002	0.014				
SKP1	-0.166	0.008	0.034	NFAT5	0.313	0.004	0.021				
TGFβ3	-0.096	0.012	0.049	PPP3R1	0.262	0.004	0.021				
NODAL	0.185	0.014	0.052	CSNK1A1	0.182	0.004	0.021				
INHBB	-0.115	0.014	0.052	WNT10B	-0.129	0.004	0.021				
CUL1	0.168	0.022	0.079	DKK2	-0.138	0.004	0.021				
CREBBP	0.150	0.028	0.096	TCF7L1	-0.155	0.004	0.021				
ZFYVE16	-0.143	0.030	0.099	CTBP2	-0.162	0.004	0.021				
EP25	-0.115	0.036	0.114	PRKX	-0.168	0.004	0.021				
RPS6KB2	-0.117	0.040	0.123	BTBRC	0.219	0.006	0.026				
RBX1	-0.130	0.044	0.130	NFATC3	0.205	0.006	0.026				
AMHR2	-0.074	0.052	0.149	SMAD3	0.203	0.006	0.026				
MAPK1	0.127	0.054	0.150	CER1	-0.063	0.006	0.026				
PPP2CA	-0.121	0.058	0.156	FRAT1	-0.167	0.006	0.026				
ACVR1C	0.141	0.062	0.161	FRAT2	-0.178	0.006	0.026				
LEFTY2	-0.046	0.074	0.187	LEF1	0.272	0.008	0.030				
NOG	0.155	0.078	0.191	FZD4	0.247	0.008	0.030				
SMAD6	0.123	0.108	0.257	PRKACB	0.195	0.008	0.030				
GDF6	-0.063	0.112	0.260	PPP2R5A	-0.165	0.008	0.030				
ZFYVE9	0.115	0.122	0.273	SKP1	-0.166	0.008	0.030				
LTFβ1	-0.206	0.124	0.273	WNT7B	0.341	0.010	0.034				
BMP2	-0.091	0.142	0.305	DAAM2	0.273	0.010	0.034				
TGFβ2	-0.063	0.146	0.306	PRICKLE2	0.239	0.010	0.034				
PPP2R1A	0.095	0.150	0.307	PPP2R5C	0.196	0.010	0.034				
SMURF1	-0.097	0.156	0.311	CND2	0.413	0.012	0.038				
TNF	-0.084	0.172	0.336	NFATC4	0.350	0.012	0.038				
THBS4	0.080	0.196	0.366	SFRP4	0.307	0.012	0.038				
ACVR2A	-0.085	0.196	0.366	CTNNA1	0.187	0.014	0.044				
RBL2	0.087	0.206	0.376	WIF1	0.300	0.020	0.060				
SMAD1	0.081	0.234	0.418	VANGL2	-0.111	0.020	0.060				
THBS1	-0.072	0.277	0.487	CUL1	0.168	0.022	0.065				
PTX2	-0.060	0.283	0.488	WNT5B	-0.122	0.024	0.070				
ID4	-0.065	0.301	0.508	AXIN1	-0.140	0.026	0.074				
PPP2R1B	-0.068	0.329	0.545	CREBBP	0.150	0.028	0.078				
SMAD4	0.056	0.411	0.607	DKK1	0.226	0.036	0.099				
RPS6KB1	0.049	0.419	0.668	RBX1	-0.130	0.044	0.118				
BMP6	0.030	0.493	0.761	CAMK2B	0.184	0.048	0.121				
BMP2	-0.047	0.509	0.761	CND3	0.155	0.048	0.121				
ID3	-0.049	0.513	0.761	MAP3K7	0.150	0.048	0.121				
THBS3	-0.050	0.505	0.761	SFRP2	-0.078	0.046	0.121				
BMP5	0.015	0.557	0.812	CSNK2A1	-0.121	0.056	0.138				
SMAD7	0.031	0.593	0.828	PPP2CA	-0.131	0.058	0.141				
RHOA	0.031	0.581	0.828	RAC2	-0.099	0.070	0.167				
INHBA	-0.040	0.597	0.828	TBL1X	0.140	0.078	0.184				
SMAD2	0.030	0.609	0.831	MAPK8	0.123	0.082	0.187				
MVC	0.034	0.645	0.866	PPP2R5B	0.115	0.082	0.187				
ACVR1	-0.036	0.663	0.866	SENP2	0.129	0.084	0.189				
RBL1	-0.037	0.665	0.866	CHP1	-0.107	0.086	0.191				
SMURF2	0.021	0.721	0.885	DVL3	0.132	0.088	0.192				
ROCK1	0.020	0.711	0.885	DKK4	0.117	0.112	0.241				
ACVR2B	0.019	0.711	0.885	MAPK10	0.114	0.120	0.255				
SP1	0.014	0.790	0.885	WNT16	0.100	0.122	0.255				
ACVR1L1	0.009	0.774	0.885	CSNK2A2	0.105	0.134	0.277				
FST	0.008	0.760	0.885	FZD5	-0.096	0.144	0.293				
INHCB	-0.019	0.770	0.885	PPP2R1A	0.095	0.150	0.301				
BMPRIIA	-0.020	0.792	0.885	FOSL1	0.087	0.152	0.301				
CHRD	-0.025	0.766	0.885	FOXL1	-0.098	0.154	0.301				
GDF7	-0.026	0.782	0.885	TCF7L2	0.096	0.160	0.309				
PPP2CB	-0.029	0.745	0.885	PPARD	-0.084	0.170	0.324				
EP300	0.014	0.826	0.893	DVL3	0.082	0.202	0.381				
MAPK3	0.012	0.830	0.893	JUN	0.090	0.208	0.385				
CDKN2B	-0.023	0.816	0.893	FZD9	0.080	0.212	0.385				
E2F4	0.000	0.894	0.938	WNT3A	0.075	0.212	0.385				
TGFβR1	-0.007	0.888	0.938	APC2	-0.063	0.234	0.420				
IFNG	-0.007	0.928	0.962	FZD8	-0.077	0.244	0.433				
BMP7	-0.012	0.980	0.984	PPP2R5D	0.083	0.265	0.456				
TFPI1	-0.014	0.978	0.984	PLCB2	-0.071	0.263	0.456				
SMAD9	-0.014	0.984	0.984	MAPK9	-0.080	0.259	0.456				
				GSK3B	0.063	0.319	0.542				
				VANGL1	0.055	0.329	0.544				
				CACBP	-0.066	0.321	0.544				
				PPP2R1B	-0.068	0.329	0.544				
				LRP6	0.062	0.335	0.544				
				CAMK2D	0.058	0.365	0.581				
				TP53	-0.062	0.363	0.581				
				DVL2	0.061	0.379	0.590				
				CHP2	-0.047	0.377	0.590				
				SMAD4	0.056	0.411	0.615				
				SFRP1	0.034	0.399	0.615				
				PSEN1	-0.053	0.403	0.615				
				NLX	-0.059	0.411	0.615				
				CSNK1A1	0.048	0.421	0.623				
				RAC3	0.049	0.435	0.638				
				PRKCB	0.031	0.449	0.652				
				FZD2	-0.047	0.461	0.660				
				PLCB1	-0.057	0.463	0.660				
				PPP3CA	0.044	0.473	0.668				
				FZD10	0.025	0.483	0.669				
				PRKACA	-0.051	0.479	0.669				
				CHDR	-0.049	0.489	0.671				
				NFATC2	-0.048	0.499	0.679				
				CAMK2A	0.022	0.517	0.697				
				TBL1XR1	0.038	0.527	0.703				
				APC	-0.048	0.531	0.703				
				FZD3	-0.042	0.559	0.734				
				RHOA	0.031	0.581	0.748				
				PPP3R2	0.019	0.577	0.748				
				RUVBL1	-0.041	0.585	0.748				
				SMAD2	0.030	0.609	0.755				
				WNT9A	0.020	0.615	0.755				
				WNT7A	0.001	0.609	0.755				
				WNT11	-0.038	0.615	0.755				
				NFATC1	-0.039	0.599	0.755				
				PRKACG	-0.036	0.635	0.767				
				SOX17	-0.036	0.633	0.767				
				MVC	0.034	0.645	0.771				
				RAC1	-0.034	0.649	0.771				
				PPP3CC	0.007	0.695	0.819				
				ROCK1	0.020	0.711	0.832				
				PRICKLE1	-0.033	0.717	0.832				
				CND1	0.034	0.731	0.842				
				PPP2CB	-0.029	0.745	0.852				
				WNT9B	-0.005	0.776	0.882				
				LRP5	0.008	0.802	0.893				
				PORCN	-0.020	0.804	0.893				



Supplementary Table 6

Low CD36 group						High CD36 group					
Gene Set Name	ES	NES	NOM p-val	FDR q-val	FWER p-val	Gene Set Name	ES	NES	NOM p-val	FDR q-val	FWER p-val
LIN_APC_TARGETS	0.481	1.873	0.000	1.000	0.604	WAKABAYASHI_ADIPOGENESIS_PPARG_RXRA_BOUND_WITH_H4K20ME1_MARK	-0.466	-2.100	0.000	0.099	0.113
LANDIS_BREAST_CANCER_PROGRESSION_UP	0.606	1.866	0.000	1.000	0.632	RUAN_RESPONSE_TO_TROGLITAZONE_UP	-0.660	-1.940	0.000	0.276	0.386
WAMUNYOKOLI_OVARIAN_CANCER_LMP_UP	0.454	1.856	0.002	1.000	0.656	GINESTIER_BREAST_CANCER_ZNF217_AMPLIFIED_UP	-0.593	-1.914	0.000	0.237	0.466
AMIT_EGF_RESPONSE_480_MCF10A	0.631	1.838	0.000	1.000	0.701	CHIANG_LIVER_CANCER_SUBCLASS_CTNNB1_UP	-0.850	-1.903	0.000	0.201	0.500
CREIGHTON_AKT1_SIGNALING_VIA_MTOR_UP	0.565	1.834	0.006	0.943	0.711	CHIANG_LIVER_CANCER_SUBCLASS_INTERFERON_DN	-0.789	-1.874	0.000	0.217	0.582
CHEN_HOXAS_TARGETS_9HR_DN	0.570	1.789	0.000	1.000	0.815	KANG_DOXORUBICIN_RESISTANCE_DN	-0.651	-1.842	0.006	0.250	0.680
BOYALT_LIVER_CANCER_SUBCLASS_G1_UP	0.586	1.778	0.012	1.000	0.837	SUZUKI_RESPONSE_TO_TSA	-0.605	-1.824	0.004	0.256	0.724
JEPSSEN_SMRT_TARGETS	0.566	1.775	0.002	1.000	0.847	SCHAEFFER_PROSTATE_DEVELOPMENT_AND_CANCER_BOX1_UP	-0.584	-1.819	0.014	0.237	0.739
LOCKWOOD_AMPLIFIED_IN_LUNG_CANCER	0.311	1.758	0.015	1.000	0.884	BOYALT_LIVER_CANCER_SUBCLASS_G1_DN	-0.747	-1.819	0.006	0.211	0.739
COULOUARN_TEMPORAL_TGFB1_SIGNATURE_UP	0.500	1.755	0.004	1.000	0.889	MOOTHA_GLYCOGEN_METABOLISM	-0.630	-1.817	0.002	0.192	0.741
RAMASWAMY_METASTASIS_UP	0.461	1.753	0.008	0.983	0.892	WANG_CLASSIC_ADIPOGENIC_TARGETS_OF_PPARG	-0.725	-1.813	0.002	0.181	0.751
LI_AMPLIFIED_IN_LUNG_CANCER	0.484	1.748	0.008	0.950	0.899	GERHOLD_ADIPOGENESIS_UP	-0.549	-1.793	0.006	0.204	0.800
DARWICHE_SKIN_TUMOR_PROMOTER_UP	0.469	1.747	0.000	0.883	0.903	BOYALT_LIVER_CANCER_SUBCLASS_G6_UP	-0.748	-1.782	0.012	0.213	0.834
TIMOFFEEVA_GROWTH_STRESS_VIA_STAT1_DN	0.666	1.738	0.006	0.901	0.913	HOSHIDA_LIVER_CANCER_SURVIVAL_DN	-0.571	-1.775	0.027	0.210	0.846
LANDIS_ERBB2_BREAST_TUMORS_324_UP	0.469	1.737	0.002	0.851	0.914	RUAN_RESPONSE_TO_TNF_DN	-0.521	-1.744	0.008	0.266	0.891
ZEMBUTSU_SENSITIVITY_TO_NIMUSTINE	0.670	1.735	0.000	0.810	0.914	YANG_MUC2_TARGETS_DUODENUM_3MO_DN	-0.757	-1.740	0.012	0.260	0.900
CHARAFE_BREAST_CANCER_LUMINAL_VS_MESENCHYMAL_UP	0.489	1.731	0.014	0.795	0.920	LUCAS_HNF4A_TARGETS_UP	-0.534	-1.739	0.027	0.248	0.901
DACOSTA_UV_RESPONSE_VIA_ERCC3_TTD_UP	0.425	1.720	0.014	0.835	0.934	STEGER_ADIPOGENESIS_UP	-0.705	-1.737	0.008	0.238	0.903
BOYALT_LIVER_CANCER_SUBCLASS_G2	0.651	1.718	0.007	0.808	0.935	CHEOK_RESPONSE_TO_HD_MTX_DN	-0.489	-1.724	0.010	0.254	0.920
DASU_IL6_SIGNALING_UP	0.614	1.709	0.004	0.833	0.940	IIZUKA_LIVER_CANCER_PROGRESSION_G2_G3_UP	-0.729	-1.723	0.028	0.243	0.921
WEIGEL_OXIDATIVE_STRESS_BY_TBH_AND_H2O2	0.545	1.709	0.004	0.795	0.940	BURTON_ADIPOGENESIS_10	-0.481	-1.722	0.021	0.234	0.921
GRAESSMANN_RESPONSE_TO_MC_AND_SERUM_DEPRIVATION_DN	0.426	1.701	0.002	0.822	0.955	RODWELL_AGING_KIDNEY_DN	-0.473	-1.720	0.006	0.227	0.924
GINESTIER_BREAST_CANCER_ZNF217_AMPLIFIED_DN	0.375	1.692	0.035	0.859	0.960	LEE_LIVER_CANCER_SURVIVAL_UP	-0.734	-1.717	0.017	0.223	0.927
POMEROY_MEDULLOBLASTOMA_DESMOPLASIC_VS_CLASSIC_DN	0.581	1.690	0.012	0.838	0.960	WOO_LIVER_CANCER_RECURRENCE_DN	-0.822	-1.714	0.008	0.220	0.933
WOO_LIVER_CANCER_RECURRENCE_UP	0.737	1.689	0.000	0.815	0.961	GUO_TARGETS_OF_IRS1_AND_IRS2	-0.522	-1.711	0.037	0.216	0.937
CHIARETTI_ACUTE_LYMPHOBLASTIC_LEUKEMIA_ZAP70	0.524	1.687	0.012	0.792	0.961	GUILLAUMOND_KLF10_TARGETS_DN	-0.644	-1.707	0.019	0.217	0.942
KAPOSI_LIVER_CANCER_MET_UP	0.638	1.685	0.006	0.780	0.964	LINDGREN_BLADDER_CANCER_WITH_LOH_IN_CHR9Q	-0.406	-1.703	0.058	0.216	0.946
CHARAFE_BREAST_CANCER_BASAL_VS_MESENCHYMAL_UP	0.613	1.685	0.010	0.754	0.964	SHEN_SMARCA2_TARGETS_UP	-0.410	-1.703	0.051	0.209	0.946
RICKMAN_METASTASIS_DN	0.466	1.682	0.021	0.746	0.965	BOYALT_LIVER_CANCER_SUBCLASS_G123_DN	-0.846	-1.703	0.008	0.202	0.946
COLDREN_GEFITINIB_RESISTANCE_DN	0.597	1.680	0.016	0.733	0.966	KIM_GERMINAL_CENTER_T_HELPER_DN	-0.582	-1.696	0.016	0.207	0.955
SMID_BREAST_CANCER_RELAPSE_IN_LUNG_UP	0.745	1.674	0.006	0.751	0.973	FRASOR_RESPONSE_TO_SERM_OR_FULVESTRANT_UP	-0.579	-1.677	0.008	0.238	0.963
MEISSNER_BRAIN_HCP_WITH_H3K27ME3	0.597	1.668	0.002	0.769	0.975	LEE_LIVER_CANCER_DENA_DN	-0.663	-1.675	0.006	0.233	0.964
FERNANDEZ_BOUND_BY_MYC	0.340	1.665	0.008	0.766	0.976	BURTON_ADIPOGENESIS_6	-0.437	-1.675	0.039	0.227	0.964
LU_TUMOR_ANGIOGENESIS_UP	0.716	1.664	0.004	0.747	0.977	LANDIS_ERBB2_BREAST_PNEOPLASTIC_DN	-0.477	-1.659	0.024	0.254	0.973
TOMLINS_METASTASIS_DN	0.569	1.664	0.019	0.731	0.977	MOOTHA_FFA_OXYDATION	-0.672	-1.655	0.078	0.257	0.973
JOHANSSON_GLIOMAGENESIS_BY_PDGF_DN	0.703	1.660	0.010	0.737	0.981	LEE_LIVER_CANCER_CIPROFIBRATE_DN	-0.629	-1.649	0.012	0.263	0.977
TOMIDA_METASTASIS_UP	0.574	1.660	0.019	0.719	0.981	SOTIRIOU_BREAST_CANCER_GRADE_1_VS_3_DN	-0.520	-1.638	0.030	0.282	0.983
BENPORATH_ES_CORE_NINE_CORRELATED	0.513	1.657	0.014	0.716	0.983	WANG_RESPONSE_TO_ANDROGEN_UP	-0.474	-1.635	0.034	0.282	0.984
ZUCCHI_METASTASIS_DN	0.591	1.656	0.029	0.705	0.984	CHIANG_LIVER_CANCER_SUBCLASS_PROLIFERATION_DN	-0.836	-1.634	0.015	0.277	0.985
NIELSEN_SYNOVIAL_SARCOMA_UP	0.737	1.655	0.008	0.697	0.986	NADLER_OBESITY_DN	-0.456	-1.618	0.030	0.310	0.990
PATTERSON_DOCETAXEL_RESISTANCE	0.592	1.653	0.010	0.691	0.986	LEE_LIVER_CANCER_E2F1_DN	-0.604	-1.609	0.040	0.325	0.993
SHETH_LIVER_CANCER_VS_TXNIP_LOSS_PAM2	0.482	1.652	0.008	0.680	0.986	CHANGOLKAR_H2AFY_TARGETS_DN	-0.502	-1.608	0.021	0.319	0.994
TURASHVILI_BREAST_DUCTAL_CARCINOMA_VS_DUCTAL_NORMAL_UP	0.706	1.648	0.010	0.688	0.986	LEE_LIVER_CANCER_MYC_TGFA_DN	-0.656	-1.608	0.032	0.313	0.994
HUPER_BREAST_BASAL_VS_LUMINAL_DN	0.591	1.648	0.012	0.676	0.987	WAKABAYASHI_ADIPOGENESIS_PPARG_RXRA_BOUND_36HR	-0.328	-1.606	0.019	0.311	0.994
LEI_MYB_TARGETS	0.434	1.646	0.012	0.668	0.987	DING_LUNG_CANCER_EXPRESSION_BY_COPY_NUMBER	-0.400	-1.605	0.078	0.307	0.995
PIONTEK_PKD1_TARGETS_DN	0.675	1.645	0.008	0.663	0.988	IIZUKA_LIVER_CANCER_PROGRESSION_L1_G1_UP	-0.698	-1.603	0.033	0.305	0.995
MEISSNER_NPC_HCP_WITH_H3K27ME3	0.631	1.643	0.002	0.659	0.989	YANG_MUC2_TARGETS_DUODENUM_6MO_DN	-0.661	-1.601	0.015	0.304	0.995
KORKOLA_TERATOMA	0.643	1.642	0.010	0.651	0.990	BOYALT_LIVER_CANCER_SUBCLASS_G12_DN	-0.851	-1.600	0.004	0.299	0.995
HAMAI_APOPTOSIS_VIA_TRAIL_DN	0.520	1.641	0.006	0.644	0.990	LEE_LIVER_CANCER_MYC_E2F1_DN	-0.655	-1.600	0.024	0.294	0.995
KANG_FLUOROURACIL_RESISTANCE_DN	0.703	1.638	0.008	0.649	0.990	NAKAYAMA_SOFT_TISSUE_TUMORS_PCA2_DN	-0.636	-1.592	0.026	0.306	0.995

Supplementary Table 7

GENE SET	Low BMI group					GENE SET	High BMI group				
	ES	NES	NOM p-val	FDR q-val	FWER p-val		ES	NES	NOM p-val	FDR q-val	FWER p-val
YAMASHITA_LIVER_CANCER_WITH_EPCAM_UP	0.597	1.910	0.008	1.000	0.478	BARRIER_COLON_CANCER_RECURRENCE_UP	-0.530	-2.041	0.002	0.581	0.197
ZHAN_VARIABLE_EARLY_DIFFERENTIATION_GENES_DN	0.501	1.908	0.002	0.521	0.481	BYSTRYKH_HEMATOPOIESIS_STEM_CELL_AND_BRAIN_QTL_CIS	-0.382	-1.968	0.002	0.628	0.346
OZEN_MIR125B1_TARGETS	0.552	1.868	0.006	0.525	0.601	WENG_POR_TARGETS_LIVER_UP	-0.714	-1.952	0.000	0.480	0.385
NIKOLSKY_BREAST_CANCER_7P22_AMPLICON	0.645	1.862	0.006	0.416	0.621	ZAMORA_NOS2_TARGETS_DN	-0.439	-1.896	0.004	0.611	0.527
BOYAULT_LIVER_CANCER_SUBCLASS_G1_UP	0.614	1.820	0.002	0.508	0.733	WAKABAYASHI_ADIPOGENESIS_PPARG_RXRA_BOUND_WITH_H4K20ME	-0.413	-1.843	0.012	0.818	0.675
CHEN_HOXA5_TARGETS_9HR_DN	0.574	1.797	0.004	0.534	0.779	GUO_TARGETS_OF_IRS1_AND_IRS2	-0.568	-1.833	0.010	0.752	0.714
POMEROY_MEDULLOBLASTOMA_PROGNOSIS_DN	0.573	1.794	0.008	0.471	0.783	DITTMER_PTHLH_TARGETS_DN	-0.412	-1.825	0.010	0.701	0.741
WELCSH_BRCA1_TARGETS_DN	0.381	1.775	0.042	0.501	0.835	WARTERS_IR_RESPONSE_5GY	-0.585	-1.820	0.002	0.651	0.754
LEE_LIVER_CANCER_SURVIVAL_DN	0.549	1.765	0.008	0.488	0.853	HOEGERKORP_CD44_TARGETS_DIRECT_UP	-0.649	-1.820	0.002	0.579	0.754
MALONEY_RESPONSE_TO_17AAG_DN	0.440	1.764	0.034	0.446	0.856	HOSHIDA_LIVER_CANCER_SURVIVAL_DN	-0.602	-1.812	0.012	0.557	0.772
ZAMORA_NOS2_TARGETS_UP	0.446	1.724	0.018	0.594	0.905	GRADE_COLON_CANCER_DN	-0.560	-1.804	0.002	0.548	0.793
BOYAULT_LIVER_CANCER_SUBCLASS_G123_UP	0.663	1.717	0.006	0.581	0.914	CAIRO_LIVER_DEVELOPMENT_DN	-0.639	-1.800	0.008	0.525	0.805
SCHLOSSER_MYC_AND_SERUM_RESPONSE_SYNERGY	0.500	1.715	0.051	0.550	0.916	BRACHAT_RESPONSE_TO_CISPLATIN	-0.586	-1.800	0.014	0.485	0.805
CHAUHAN_RESPONSE_TO_METHOXYESTRADIOL_UP	0.513	1.712	0.017	0.526	0.920	KYNG_NORMAL_AGING_DN	-0.525	-1.799	0.002	0.452	0.809
RAMASWAMY_METASTASIS_UP	0.439	1.693	0.030	0.590	0.941	ACEVEDO_NORMAL_TISSUE_ADJACENT_TO_LIVER_TUMOR_UP	-0.407	-1.790	0.008	0.463	0.830
PETROVA_PROX1_TARGETS_UP	0.694	1.692	0.008	0.561	0.942	UEDA_PERIFERAL_CLOCK	-0.456	-1.784	0.017	0.461	0.847
PARK_HSC_AND_MULTIPOTENT_PROGENITORS	0.364	1.690	0.014	0.536	0.943	PIONTEK_PKD1_TARGETS_UP	-0.702	-1.772	0.004	0.488	0.868
AGUIRRE_PANCREATIC_CANCER_COPY_NUMBER_UP	0.306	1.674	0.028	0.583	0.956	GAZDA_DIAMOND_BLACKFAN_ANEMIA_ERYTHROID_UP	-0.550	-1.761	0.008	0.512	0.887
PEART_HDAC_PROLIFERATION_CLUSTER_UP	0.469	1.647	0.060	0.711	0.971	GROSS_HYPOXIA_VIA_ELK3_ONLY_UP	-0.630	-1.758	0.011	0.504	0.894
PRAMOONJAGO_SOX4_TARGETS_DN	0.472	1.643	0.020	0.698	0.974	HELLER_SILENCED_BY_METHYLATION_DN	-0.505	-1.753	0.002	0.507	0.900
MUELLER_PLURINET	0.439	1.633	0.056	0.723	0.981	FOURNIER_ACINAR_DEVELOPMENT_EARLY_UP	-0.627	-1.749	0.025	0.500	0.903
SANA_RESPONSE_TO_IFNG_DN	0.395	1.607	0.030	0.870	0.989	BOCHKIS_FOXA2_TARGETS	-0.435	-1.748	0.012	0.483	0.905
HSIAO_HOUSEKEEPING_GENES	0.329	1.606	0.144	0.837	0.989	PICCALUGA_ANGIOIMMUNOBLASTIC_LYMPHOMA_DN	-0.504	-1.748	0.024	0.463	0.906
NADERI_BREAST_CANCER_PROGNOSIS_UP	0.671	1.606	0.017	0.807	0.989	CHIANG_LIVER_CANCER_SUBCLASS_UNANNOTATED_UP	-0.710	-1.735	0.000	0.494	0.924
WONG_EMBRYONIC_STEM_CELL_CORE	0.456	1.604	0.089	0.786	0.990	HOWLIN_CITED1_TARGETS_2_DN	-0.640	-1.729	0.010	0.508	0.930
ZHANG_RESPONSE_TO_CANTHARIDIN_DN	0.399	1.603	0.082	0.763	0.990	HAHTOLA_MYCOSIS_FUNGOIDES_UP	-0.617	-1.721	0.008	0.527	0.942
COLLIS_PRKDC_SUBSTRATES	0.490	1.602	0.046	0.742	0.990	SERVITJA_LIVER_HNF1A_TARGETS_DN	-0.632	-1.718	0.000	0.521	0.946
LIN_APC_TARGETS	0.416	1.599	0.032	0.732	0.990	GERHOLD_ADIPOGENESIS_UP	-0.500	-1.715	0.018	0.517	0.948
BILANGES_SERUM_AND_RAPAMYCIN_SENSITIVE_GENES	0.541	1.599	0.091	0.710	0.990	LEE_LIVER_CANCER_CIPROFIBRATE_UP	-0.551	-1.713	0.002	0.510	0.950
BERTUCCI_INVASIVE_CARCINOMA_DUCTAL_VS_LOBULAR_UP	0.512	1.583	0.025	0.782	0.992	YAMASHITA_LIVER_CANCER_STEM_CELL_DN	-0.773	-1.703	0.002	0.540	0.956
FRASOR_RESPONSE_TO_SERM_OR_FULVESTRANT_DN	0.667	1.583	0.045	0.757	0.992	COULOUARN_TEMPORAL_TGFB1_SIGNATURE_DN	-0.500	-1.700	0.033	0.535	0.961
ZEMBUTSU_SENSITIVITY_TO_CYCLOPHOSPHAMIDE	0.601	1.581	0.032	0.741	0.992	VANLOO_SP3_TARGETS_DN	-0.494	-1.691	0.002	0.565	0.968
GRADE_COLON_AND_RECTAL_CANCER_UP	0.349	1.580	0.066	0.727	0.992	VANDELSUIS_COMMD1_TARGETS_GROUP_4_UP	-0.630	-1.686	0.002	0.576	0.975
NIKOLSKY_BREAST_CANCER_20Q12_Q13_AMPLICON	0.465	1.577	0.028	0.724	0.992	WENG_POR_DOSAGE	-0.715	-1.684	0.020	0.566	0.976
GARCIA_TARGETS_OF_FLI1_AND_DAX1_DN	0.447	1.571	0.053	0.736	0.992	DAUER_STAT3_TARGETS_UP	-0.613	-1.677	0.024	0.586	0.976
HEDENFALK_BREAST_CANCER_HEREDITARY_VS_SPORADIC	0.367	1.571	0.045	0.717	0.992	OHGUCHI_LIVER_HNF4A_TARGETS_DN	-0.716	-1.673	0.010	0.592	0.980
LIAO_HAVE_SOX4_BINDING_SITES	0.628	1.561	0.010	0.753	0.993	FLECHNER_PBL_KIDNEY_TRANSPLANT_OK_VS_DONOR_DN	-0.448	-1.669	0.036	0.595	0.981
OXFORD_RALA_OR_RALB_TARGETS_UP	0.678	1.557	0.054	0.755	0.993	ONDER_CDH1_TARGETS_1_UP	-0.446	-1.659	0.008	0.634	0.983
WU_APOPTOSIS_BY_CDKN1A_VIA_TP53	0.737	1.554	0.047	0.752	0.993	GROSS_HYPOXIA_VIA_ELK3_AND_HIF1A_UP	-0.469	-1.656	0.025	0.636	0.983
MODY_HIPPOCAMPUS_PRENATAL	0.481	1.548	0.081	0.764	0.994	HOSHIDA_LIVER_CANCER_SUBCLASS_S3	-0.677	-1.652	0.047	0.647	0.988
SONG_TARGETS_OF_IE86_CMV_PROTEIN	0.664	1.546	0.067	0.758	0.994	SMIRNOV_RESPONSE_TO_IR_6HR_UP	-0.399	-1.650	0.020	0.640	0.988
IRITANI_MAD1_TARGETS_DN	0.419	1.546	0.112	0.743	0.994	LUCAS_HNF4A_TARGETS_UP	-0.515	-1.644	0.045	0.655	0.991
BLUM_RESPONSE_TO_SALIRASIB_DN	0.479	1.545	0.081	0.730	0.995	LEE_LIVER_CANCER_MYC_TGFA_DN	-0.668	-1.643	0.018	0.647	0.992
NGO_MALIGNANT_GLIOMA_1P_LOH	0.491	1.544	0.073	0.718	0.995	GOLDRATH_IMMUNE_MEMORY	-0.491	-1.643	0.029	0.633	0.992
LE_EGR2_TARGETS_UP	0.611	1.544	0.061	0.705	0.995	YAMASHITA_LIVER_CANCER_WITH_EPCAM_DN	-0.845	-1.640	0.010	0.631	0.992
CROMER_METASTASIS_DN	0.449	1.540	0.055	0.707	0.995	BOYAULT_LIVER_CANCER_SUBCLASS_G1_DN	-0.688	-1.640	0.051	0.620	0.992
LU_EZH2_TARGETS_UP	0.395	1.539	0.062	0.698	0.995	PACHER_TARGETS_OF_IGF1_AND_IGF2_UP	-0.542	-1.639	0.004	0.608	0.992
KIM_ALL_DISORDERS_DURATION_CORR_DN	0.382	1.533	0.095	0.713	0.996	ZHENG_FOXP3_TARGETS_UP	-0.675	-1.638	0.019	0.600	0.992
LOCKWOOD_AMPLIFIED_IN_LUNG_CANCER	0.271	1.532	0.074	0.705	0.997	FALVELLA_SMOKERS_WITH_LUNG_CANCER	-0.487	-1.638	0.010	0.593	0.992
TOMIDA_METASTASIS_UP	0.532	1.529	0.046	0.705	0.997	LIANG_HEMATOPOIESIS_STEM_CELL_NUMBER_SMALL_VS_HUGE_UP	-0.473	-1.638	0.014	0.582	0.992

**Figure 1: Fatty acid uptake and EMT markers in TCGA liver cancer dataset.** A. 158 samples from the TCGA LIHC database were analyzed to determine the effect of patient's BMI on EMT and FA uptake gene expression. Box plot showing comparison of EMT scores, mRNA expression levels of hepatic FA uptake genes and *CD36* in groups of patients with BMI < 25 (Low BMI, n=75) or  $\geq 25$  (High BMI, n=83). P-values indicate significance levels from two-tailed Student's T-test. B. Scatter plots showing correlation between BMI (X-axis) and EMT score, *CD36*, *ZEB1* or *FNI* (Y-axis). The solid red line indicates linear fit, with 95% confidence intervals indicated by dotted black lines. *r* indicates Pearson's correlation coefficient and p-values indicate significance of correlation (two-tailed), with the red boxes marking significant associations from the multivariate regression analysis. C. Heatmap showing relative expression levels of hepatic fatty acid uptake genes and EMT genes in the TCGA liver cancer dataset. Gene clusters (vertical axis) were obtained by hierarchical clustering and samples (horizontal axis) were ordered according to the EMT score. D. Scatter plot showing association between the fatty acid uptake genes (Y-axis) and EMT score (X-axis) drawn from 158 patient samples in the TCGA dataset. The solid red line indicates linear fit, with 95% confidence intervals indicated by dotted black lines. *r* indicates Pearson's correlation coefficient and p-values indicate significance of correlation (two-tailed), with the red boxes marking significant associations from the multivariate regression analysis (n=158). Clinical data for each patient is available in Supplementary Table 1 (Bonferroni adjusted p-value cut-off for the analysis = 0.0016).

**Figure 2: CD36 and EMT marker expression in human HCC tumors.** A. Western blots showing expression levels of CD36 and various EMT markers in tumor samples grouped according to BMI. High BMI group (n=8) represents tumor samples obtained from individuals with BMI  $\geq 30$  and low BMI group (n=8) indicates individuals with BMI  $\leq 25$ . Equal amounts of sample (40 $\mu$ g) were loaded in each well, run under identical conditions and blotted with specific primary antibodies against the indicated proteins. For clarity, blots have been cropped to show relevant bands (full length blots are presented in Supplementary Figure 3) B. Expression levels of proteins were determined by quantifying the

background-subtracted band intensities normalized to GAPDH. Each dot represents relative expression levels of individual samples, with the horizontal bar indicating the median of the distribution. P-values indicate significance of difference in means between low BMI and high BMI groups determined by Mann-Whitney U test, with red boxes marking significant associations from multivariate regression analysis. C. Scatter plot showing association between CD36 (X-axis) and EMT marker (Y-axis) expression. The solid lines indicate linear fit and the dotted lines indicate 95% confidence intervals.  $r$  indicates Pearson's correlation coefficient and p-values indicate significance of correlation (two-tailed), with red boxes marking significant associations from multivariate regression analysis (n=16). Specific clinical data for each patient is available in Supplementary Table 3.

**Figure 3: PA mediated EMT induction.** A. Scratch-wound cell migration assays with HepG2 and Hep3B cells treated with different concentrations of PA (0.1mM to 0.4mM) and BSA (control). The plot indicates average number of migrating cells in the wound area at 24 and 48 hours following 5-day treatment normalized to 0 hour time point (n=3). P-values indicate the significance levels compared to BSA at a given time point determined by Tukey's test following one-way ANOVA. B. Phase contrast microscopy images of HepG2 and Hep3B cells treated with BSA or PA (0.3mM) at 48 hours (40X magnification, scale bar=50 $\mu$ m). C. Confocal images of HepG2 demonstrating changes in morphology upon PA treatment. Keratin 18 and nuclear staining are indicated by green and blue fluorescence respectively. (40X magnification, scale bar=100 $\mu$ m). D. Modified Boyden's chamber assays with HepG2 and Hep3B cells. The bar graph indicates the average number of migrating or invading cells ( $\pm$ SEM, Standard Error of the Mean) counted in 5 fields of view per insert (n=3). P-values indicate significance levels determined by Student's t-test (two-tailed). E. Bright field images at 5X (scale bar=400 $\mu$ m) magnification showing fragmentation in monolayers of BSA or PA treated Hep3B or HepG2 cells following dispase treatment and application of mechanical stress. F. Particle analysis following dispase assay. Bar graphs showing average particle count and fragment diameter ( $\pm$ SEM) determined from 5

independent images panels obtained after dispase treatment and applying mechanical stress to BSA or PA treated HepG2 and Hep3B cells. P-values indicate significance levels determined by Student's t-test.

**Figure 4: Cytotoxicity vs. metabolic activity.** A. Bar graph showing average cytotoxicity ( $\pm$ SEM) determined using LDH assay in HepG2 or Hep3B cells following 5 day (with serum) and 2 day (without serum) treatment with BSA or PA at different concentrations (n=3). P-values indicate significance levels comparing average LDH release in PA treated cells with BSA treated cells determined by Student's t-test (two tailed). B. Bar graph showing the relative metabolic activity represented by average fluorescence ( $\pm$ SEM) from reduced AlamarBlue reagent (resazurin) in HepG2 or Hep3B cells following 5 day treatment (with serum) and 2 day (without serum) with BSA or PA (n=3). P-values indicate significance levels determined by Student's t-test (two tailed). Numbers above bars indicate the percentage of proliferating cells at 48 hours compared to 0 hours. C. Neutral lipids and fatty acids in HepG2 or Hep3B cells were stained with Oil Red O following 5 day (with serum) and 2 day (without serum) treatment with BSA or PA. Bright-field microscopy images were recorded at 40X magnification (scale bar=50 $\mu$ m). D. Relative levels of lipids and fatty acids in BSA and PA treated cells were quantified by eluting the Oil Red O dye and measuring relative absorbance at 500nm. Bar graph shows average absorbance ( $\pm$ SEM) in BSA and PA treated cells. P-values indicate significance levels comparing average absorbance in BSA or PA treated cells determined by Student's t-test (two tailed).

**Figure 5: Population effect of PA on EMT marker expression.** A. Density plots showing distribution of cells co-stained with zombie violet (Y-axis) and either CDH, DSP or VIM (X-axis) in HepG2 cells treated with BSA or PA (0.3mM). The bars represent staining thresholds for zombie violet (horizontal bar) or the protein markers (vertical bar). Lower left quadrant represents background staining, upper left quadrant represents cells stained with only zombie violet, upper right quadrant represent cells co-stained with zombie violet and protein marker and lower right quadrant represent cells stained with protein marker only. The numbers in the plot represent the percentage of total cells within that quadrant. B. Confocal images showing **specific regions with altered** expression levels of CDH and VIM in HepG2 and

Hep3B cells. Blue indicates nuclear staining and green indicates CDH or VIM staining. Images were recorded at 40X with identical exposure and PMT settings maintained between BSA and PA treated cells for a given marker (scale bar = 100 $\mu$ m). C Bar graph showing fold-change in mRNA expression levels of various EMT transcription factors determined by qRT-PCR in PA (0.3mM) treated HepG2 cells compared to corresponding expression levels in BSA treated cells (*GAPDH* normalized). P-values indicate significance levels compared to BSA determined by Student's t-test (two tailed), n = 3.

**Figure 6: EMT pathways induced by PA.** A. Heatmap showing relative fold-change in mRNA expression levels of various EMT-related genes in PA (0.3mM) vs. BSA treated cells measured by EMT-array. The enlarged heatmap shows fold change in expression levels of the components of TGF $\beta$ - and Wnt-signaling pathways included in the array. B. The top 20 genes ranked according by fold-change in the array were enriched for KEGG pathways. The table shows the term (KEGG pathway) enriched, number and percentage of genes in the input set belonging to the pathway and significance levels of enrichment. C-F. Confocal images showing expression of  $\beta$ -catenin or SMAD2/3 (green) and nuclei (blue) in HepG2 and Hep3B cells treated with BSA or PA (0.3mM). The overlap panel shows pixels where both green and blue fluorescence co-localize, therefore indicating cells displaying translocation of  $\beta$ -catenin or SMAD2/3 transcription factors to the nucleus. Images were recorded at 40X with identical exposure and PMT settings maintained between BSA and PA treated cells for a given marker (scale bar = 100 $\mu$ m).

**Figure 7: Correlation matrix heatmaps showing the association between mRNA expression z-scores (TCGA) of *CD36* and** A. Wnt signaling pathway genes (KEGG) B. TGF beta signaling pathway (KEGG) C. PPARs and transcriptional mediators of inflammatory pathways known to be induced by free fatty acids. Genes are clustered with average linkage hierarchical clustering using 1-Pearson's correlation as distance metric. Black boxes in A and B show the nearest neighbors of *CD36* with strong positive correlation, with enlarged list showing the names of genes in that cluster. D. Overview of the influence of elevated free fatty acid uptake on cell signaling pathways resulting in the induction of EMT program. Red

ovals represent genes that were upregulated in vitro in PA treated HCC cells; orange ovals represent genes that show positive correlation with *CD36* in the TCGA dataset; white ovals represent genes that did not show a significant correlation with *CD36* in the TCGA dataset. Dashed black arrows show transport/translocation, solid black arrows and bar-headed lines indicate positive and negative regulation respectively. Blue arrows indicate consequence of activation of the proteins in context of the EMT program.

**Figure 8: CD36 and TGF-beta/Wnt-signaling mediate PA effects.** A. Western blots showing expression of CDH and VIM in HepG2 cells treated with BSA or PA (0.3mM) for 5 days with serum. Additionally, the cells were co-treated with either 100 $\mu$ M SSO (CD36 inhibitor) or DMSO (solvent control). Equal amounts of sample (40 $\mu$ g) were loaded in each well, run under identical conditions and blotted with specific primary antibodies against the indicated proteins. For clarity, blots have been cropped to show relevant bands (full length blots are presented in Supplementary Figure 4). B-C. Bar graphs showing quantification of blots indicating expression levels of CDH and VIM normalized to GAPDH in BSA or PA treated cells (n=3). P-values indicate significance levels comparing SSO treated (+SSO) BSA or PA treated cells with DMSO control (-SSO) cells determined by Student's t-test (two tailed). D. HepG2 cells were treated with PA (0.3mM) and DMSO (control),  $\beta$ -catenin/Tcf inhibitor III (100nM) or TGF- $\beta$ 1 RI kinase inhibitor (50nM) in presence of serum for 5-days, followed by wound-healing assay in serum-free media over 48 hours. Bar graph indicates average wound closure (wound closure = 100 - % open wound area) normalized to 0 hour time point (n=3). P-value indicates significance levels comparing the open wound area in inhibitor treated cells with control cells determined by Student's t-test (two tailed). E. HepG2 cells were treated with PA (0.3mM) and DMSO (control), CD36 inhibitor SSO (100 $\mu$ M) or porcupine inhibitor LGK974 (100nM) in presence of serum for 5-days, followed by Boyden's chamber migration assay over 48 hours in serum-free media, with 10% FBS containing regular medium as chemoattractant. Bar graph indicates the average number of migrating cells (n=3). P-value

indicates significance levels comparing the number of migrating cells with inhibitor treatment against control, determined by Student's t-test (two tailed).



**Supplementary Figure 1: Differential effects of FFAs on migration**

**Supplementary Figure 2:** mRNA expression levels of Hedgehog ligand *SHH* and downstream transcription factor *GLI1* in PA vs. BSA treated HepG2 cells

**Supplementary Figure 3:** Uncropped western blot images supporting Figure 2A

**Supplementary Figure 4:** Uncropped western blot images supporting Figure 8A

**Supplementary Figure 5: Flow cytometry gating and intensity plots**

**Supplementary Table 1:** Log2 transformed TCGA LIHC data from cBioPortal for FA Uptake Genes: CD36, FABP1, FABP4, FABP5, SLC27A2, SLC27A5; Mesenchymal Genes: CDH2, FN1, SNAI1, SNAI2, TWIST1, TWIST2, VIM, ZEB1, ZEB2; Epithelial Genes: CDH1, CLDN4, CLDN7, MUC1, TJP3; EMT scores; and Patient clinical data: Age, gender, height, weight, BMI, EMT score and pathological (TNM) staging

**Supplementary Table 2:** Pearson's correlation coefficient and p-values (two-tailed) between EMT score and FA uptake genes, BMI and FA uptake genes, and BMI and EMT genes (Bonferroni adjusted p-value cut-off = 0.0016)

**Supplementary Table 3:** Clinical information including BMI, sex, grade and pathological staging information and results of western blot quantification for the corresponding samples

**Supplementary Table 3:** Palmitate, oleate and linoleic acid free fatty acid levels in HCC vs. normal cases

**Supplementary Table 4:** Fold-change in gene expression levels of EMT genes in PA vs. BSA treated HepG2 or Hep3B cells. Genes were ranked by fold-change and the highlighted genes (top-20) were used for KEGG pathway enrichment analysis. Direct transcriptional targets of TGF and WNT signaling pathways are marked.

**Supplementary Table 5:** Correlation analysis comparing expression profile of CD36 in TCGA HCC dataset with KEGG Wnt/TGFB signaling pathways genes, PPAR genes and the transcriptional effectors of inflammatory pathways known to be induced by free fatty acids.

**Supplementary Table 6:** Gene set enrichment analysis of TCGA HCC data with patients stratified into low CD36 and high CD36 expression clusters (only the top 50 gene sets are listed)

**Supplementary Table 7:** Gene set enrichment analysis of TCGA HCC data with patients stratified into low BMI and high BMI groups (only the top 50 gene sets are listed)